Final Report

DE-FC26-05NT42517

Project No. 42517 - Delsulfurization of High-Sulfur Jet Fuels by Adsorption and Ultrasound-Assisted Sorbent Regeneration

Submitted to Dr. Ayyakkannu (Mani) Manivannan, Project Manager

By Yuhe Wang, Liping Ma and Ralph T. Yang

Department of Chemical Engineering

University of Michigan

Ann Arbor, MI 48109

Period covered by this report: November 1, 2005 - October 31, 2006

November 20, 2006

Disclaimer

Abstract

This work was conducted for the department of Energy. In this work, we developed a class of new sorbents that were highly sulfur sepective and had high sulfur capacities. The study consisted of two sections. Development of the new sorbents is described in Section 1, and Section was a fundamental study, conducted for a better understanding for desulfurization of jet fuels. More details of the results are given blow separately for the two sections.

Section 1: Desulfurization of Model Jet Fuels by Adsorption on Carbon-based Sorbents and Ultrasound-Assisted Sorbent Regeneration

Several high-sulfur-capacity carbon-based adsorbents, CuCl/AC, $PdCl_2$/AC, and Pd/AC (where AC denotes activated carbon), were studied for desulfurization of a model jet fuel by selective adsorption of thiophenic molecules. The model jet fuel (150 ppmw-S BT and 250 ppmw-S MBT in 19.75 wt% benzene + 80 wt% *n*-octane containing 700 ppmw naphthalene) was formulated such that it represented all jet fuels well. In addition, a commercial jet fuel, JP-5 was included in the tests. Comparisons with γ-Al_2O_3 support and desulfurization of a commercial jet fuel were also studied. The results showed that the selective sulfur adsorption capacity of $PdCl_2$ was higher than that of CuCl and Pd^0, in agreement with molecular orbital results. It was also found that the activated carbon is the best support for π-complexation sorbents to remove sulfur-containing compounds, i.e. benzothiophene and methylbenzothiophene. Among all the adsorbents studied, $PdCl_2$/AC had the highest capacity for desulfurization. A significant synergistic effect was

observed between the carbon substrate and the supported π-complexation sorbent, and this effect was explained by a geometric effect. The saturated sorbent was regenerated by desorption assisted by ultrasound with a solvent of 30 wt% benzene and 70 wt% *n*-octane. The results showed that the amount of sulfur desorbed was higher with ultrasound, 65 wt% desorption vs. 45 wt% without ultrasound in a static system at 50 °C.

Section 2: Selective Adsorption of Sulfur Compounds: Isotherms, Heats and Relationship between Adsorption from Vapor and Liquid Solution

This was a basic study in order to understand and better design sorbents for desulfurization of jet fuels. Adsorption isotherms were measured for thiophenic sulfur compounds, thiophene (T), benzothiopnene (BT), 2-methyl benzothiophene (2-MBT) and dibenzothiophene (DBT), from their binary solutions in *n*-octane. Two sulfur-selective, π-complexation sorbents were studied: Cu(I)-Y zeolite and $PdCl_2$ impregnated on activated carbon ($PdCl_2$/AC). Vapor-phase isotherms of *n*-octane and thiophene were also measured. The selectivity of adsorption from liquid solutions followed the order of: T < BT < 2-MBT < DBT for $PdCl_2$/AC, and T < DBT < 2-MBT < BT for Cu(I)-Y zeolite. The adsorption bond energies, which approximate the heats of vapor-phase adsorption, followed the order: T < BT < 2-MBT < DBT. This order was not followed for adsorption from liquid solutions on Cu-Y zeolite. The heats of adsorption were obtained by the temperature dependence of the isotherms. A simple theory was proposed for estimating the relationship between the heat of adsorption from liquid solution and that from vapor phase. The experimental results were in fair agreement with the theory.

Table of Contents

Section 1: Desulfurization of Model Jet Fuels by Adsorption on Carbon-based Sorbents and Ultrasound-Assisted Sorbent Regeneration

1. Introduction

The jet fuels are strategic fuels for the military and considered by many as an excellent hydrogen source choice for future fuel cells.[1,2] Removal of sulfur containing compounds is an important operation in petroleum refining, and is achieved by catalytic processes operated at high pressures and elevated temperatures. Today, refineries rely on hydrodesulfurization (HDS) processes to reduce sulfur levels from commercial fuels, but achieving deep-desulfurization levels would require increasing existing reactor sizes and increasing hydrogen consumption.[3] There has been much recent interest in developing sorbents for selective desulfurization.[4-9] We have recently developed a class of sorbents that rely on π-complexation bonding to selectively remove organosulfur molecules from commercial fuels.[10-16] These sorbents were prepared by using several ion-exchange techniques to introduce d-block metals into zeolites, including Ag^{+}, Cu^{+}, Ni^{2+}, and Zn^{2+}. These ion-exchanged materials are capable of producing fuels with a total sulfur concentration of less than 1 ppmw. In particular, the Cu(I)-Y zeolite (vapor-phase ion exchange or VPIE) showed the highest selectivity and capacity for sulfur from the transportation fuels.[1,10]

A caveat is in order concerning the π-complexation sorbents, especially Cu(I)Y. First, Cu(I)Y is unstable; it is easily oxidized to Cu(II)Y by air, moisture or other oxidants; and once oxidized, it loses its superior sulfur selectivity and capacity. Any missteps in the experiment could lead to some degrees of oxidation. For example, the auto-reduction step (to reduce Cu(II)Y to Cu(I)Y in an inert atmosphere at 450°C) requires more than 15 hours to complete (we typically used 18 hours). Shorter reduction

times in our laboratory[17] as well as in other laboratories[18,19] resulted in incomplete reduction and lower sulfur capacities. Moreover, a number of fuel constituents could have detrimental effects as demonstrated in our recent work, such as organo-nitrogen compounds,[14] moisture and added oxygenates.

Some preliminary tests in our laboratory indicate that the Pd doped on Y zeolite sorbent showed excellent adsorption performance for removing sulfur from EC diesel (9.2 ppmw-S). In addition, our previous studies have shown that activated carbon in a guard bed can improve the adsorptive performance of Cu(I)-Y adsorbent[15,20]. Studies by other groups were also reported regarding desulfurization and denitrogenation of liquid hydrocarbon fuels by adsorption over activated carbons.[4,21-25]

Pure activated carbon and activated carbon impregnated with metal halides (AgCl, CuCl, CuBr, CuI, $FeCl_2$, $FeCl_3$, $NiCl_2$, $PdCl_2$ and $ZnCl_2$) were studied for adsorbing CO in the study of Tamon, et al.[27] The carbons impregnated with CuCl, CuBr, CuI, and $PdCl_2$ yielded large adsorption capacities compared with the unimpregnated carbon. In particular, the amounts of CO adsorbed on $PdCl_2$- and CuCl-impregnated carbons were approximately twenty and eight times, respectively, that of the unimpregnated carbon. This indicates that the impregnation of metal halides is effective in increasing the adsorption ability of CO on the carbon-based adsorbents.

Most recently, we have found that $PdCl_2$/AC was an excellent sorbent for desulfurizing very high-sulfur commercial jet fuels such as JP-5 that contained 1172 ppmw S.[28] For JP-5, significant breakthrough occurred at about 6.0 ml/g with $PdCl_2$/AC, far greater than all other known sorbents. This finding prompted us to undertake an in-depth study of the π-complexation sorbents that are supported on activated carbon.

Because of the complexities involved in the commercial jet fuels (i.e., each fuel contains more that 150 different compounds), a model jet fuel was used for this study in order to obtain a basic understanding. The regeneration of the $PdCl_2$/AC sorbent using ultrasound technique was also studied.

2. Experimental Method

2.1 Adsorbent preparation

The starting adsorbent material used in this study was activated carbon (AC, Type PCB, Calgon Carbon Corporation) and activated alumina (γ-Al_2O_3, Type PSD, ALCOA Industrial Chemicals).

CuCl/AC and $PdCl_2$/AC sorbents were prepared by impregnating activated carbon (100-140 mesh) with metal halides.[27] A known amount of metal halide (2.15 g CuCl or $PdCl_2$, Sigma-Aldrich) was magnetically stirred in 1 M HCl aqueous solution of 15 ml volume under a dry helium atmosphere at room temperature, and then 5 g of activated carbon was added to the mixture. After 24 h, the sample was washed with deionized water until the pH of the water became around 5.0, and the sample was dried in helium at 130 ºC for 12 h. After that, a CuCl/AC or $PdCl_2$/AC sorbent was obtained. Before the desulfurization experiment, the sorbents were activated *in situ* in a quartz adsorber under ultra-pure helium using a heating rate of 1 ºC/min from room temperature to 120 ºC and held at that temperature for 6 h.

A standard impregnation method was used to prepare Pd metal supported on AC (100-140 mesh).[29] The steps were as follows: add 3 g activated carbon into 10 ml of 2-butanol and heating the solution to 80 ºC under stirring to obtain solution (I); add 2.1 g $Pd(NO_3)_2 \cdot xH_2O$ (Sigma-Aldrich) into 10 ml 2-butanol and stirring the solution for 30 min

to get solution (II). Then add solution (II) dropwise into solution (I) at 80 ºC under stirring. The sample was air-dried at 120 ºC for 16 h. Before its use in adsorptive desurlfurization, the precursor was reduced directly in a 60 cm^3/min steam of ultra-pure dry H_2 at 1 ºC/min to 250 ºC, which was maintained for at least 12 h. Then the Pd/AC sorbent was obtained *in situ* for the desulfurization of fuels.

The $PdCl_2/\gamma$-Al_2O_3 sorbent was prepared using the technique of spontaneous monolayer dispersion.[2,30] That the supported salts are indeed spread into a monolayer has been proven by using a number of techniques.[2,30] The γ-Al_2O_3 powder (100-140 mesh) was first activated in a dry helium atmosphere at 350 ºC for 2 h. Afterwards, 1.0 g γ-Al_2O_3 and 0.493 g $PdCl_2$ (Sigma-Aldrich) were mixed thoroughly and then the mixture was placed in a quartz tube for heat treatment at 450 ºC in He. After 24 h of heat treatment, the monolayer supported $PdCl_2/\gamma$-Al_2O_3 sorbent was obtained. Before its use in adsorptive desurlfurization, the sorbent was pretreated in a ultra-pure helium at 1 ºC/min to 350 ºC, which was maintained for 6 h.

2.2 Adsorbent characterization

The BET surface areas of the samples were measured by physical adsorption of N_2 at 77K using Micromeritics ASAP 2010. The loadings of CuCl or $PdCl_2$ on the activated carbon were measured by burning the samples in flowing oxygen (50 ml/min) at a heating rate of 10 ºC/min. A TGA thermogravimetric analyzer (Shimadzu TGA-50) was used for the measurements. The combustion experiments were carried out for the supported sorbents (CuCl/AC and $PdCl_2$/AC) as well as the activated carbon support and pure metal salts (CuCl or $PdCl_2$). The loadings of metal salts on activated carbon could then be calculated by the comparison of the "ash" contents between the sorbents,

activated carbon and pure metal salts. The physical properties of different sorbents are listed in Table 1.

Pore size distribution was also analyzed by N_2 adsorption at 77K. The Horvath-Kawazoe method was used for calculating the micropore sizes.

Chemisorption of CO at 35 ºC was measured using the Micromeritics ASAP 2020 system. It was used to characterize the dispersion of $PdCl_2$ on activated carbon.

2.3 Reagents and standards

The major sulfur-containing compounds in jet fuels are benzothiophene and its methylated derivatives.[1,31,32] Essentially no thiophenes and dibenzothiophenes are found. A model jet fuel was prepared according to the main sulfur-containing compounds in commercial jet fuels, with the composition given in Table 2. Benzothiophene (BT) and 2-methybenzothiophene (MBT), from Sigma-Aldrich, were used without further purification.

2.4 Fixed-bed adsorption/breakthrough experiments

All dynamic adsorption or breakthrough experiments were performed in a vertical custom-made quartz adsorber equipped with a supporting glass frit as described elsewhere.[10,12-16] The setup consisted of a low-flow liquid pump, feed tanks, and a heating element. Initially, the sorbents were loaded inside the adsorber, and pretreated *in situ* using dry gases to avoid exposure to atmospheric moisture. The gases used for activation were pretreated inline before contacting the sorbent using a column of 3A-type zeolite. After activation treatment, the sorbent bed was washed with a sulfur free hydrocarbon (e.g. *n*-octane) to remove any entrapped gas. After allowing the liquid hydrocarbon head to disappear, the fuel was allowed to contact the bed in a down-flow direction. The

effluent was sampled periodically until saturation was achieved, which depended on the adsorption dynamics and the amount of adsorbent.

Breakthrough adsorption curves were generated by plotting the transient total sulfur concentration normalized by the feed total sulfur concentration versus cumulative fuel volume normalized by total bed weight. The adsorption amounts (normalized per adsorbent weight) were obtained after solving the following equation: [2,27]

$$q_{\substack{breakthrough \\ or\ saturation}} = \left(\frac{\dot{v}}{m_{adsorbent}}\right)\left(\frac{\rho_{fuel} X_i}{MW_{sulfur}}\right)\int_0^t \left[1 - \frac{C(t)}{C_i}\right] dt$$

where q is the total sulfur adsorbed amount (mmol/g), $\dot{v}$ is the feed volumetric flow rate (cm^3/min), ρ_{fuel} is the fuel density (g/cm^3) at room temperature, X_i is the total sulfur fraction (by weight) in the feed, C_i is the total sulfur concentration in the feed (ppmw-S), $m_{adsorbent}$ is the weight of the sorbent bed (g), MW_{sulfur} the molecular weight of sulfur, $C(t)$ the effluent total sulfur concentration (ppmw-S) at time t (min). The breakthrough adsorption amounts were obtained at the point where the fuel total sulfur concentration was less than approximately 1 ppmw-S.

2.5 Gas chromatograph analysis

All the samples collected during the breakthrough experiments were analyzed using a Shimadzu GC-17A v3 unit equipped with an EC-5 capillary column and a flame photometric detector (FPD). More details on the GC analysis could be found elsewhere.[12-16] For standards, stock solutions consisting of benzothiophene (BT) and 2-methylbenzothiophene (MBT) in sulfur-free *n*-octane were further diluted sequentially to known concentrations and then injected for elution time determination.

2.6 Regeneration

In this work, the feasibility for desorption of sulfur compounds from $PdCl_2$/AC sorbent was investigated in a batch mode. The spent sorbent was regenerated by adding 50 ml of a mixture of benzene (30 wt%) and *n*-octane (70 wt%) in a container maintained at different temperatures. The desorption was performed with and without ultrasound. More details can be found elsewhere.[2,33]

3. Results and discussion

3.1 Sorbent characterization

Figure 1 shows the isotherm of CO adsorption on the monolayer $PdCl_2/\gamma$-Al_2O_3. Based on the isotherm, the saturation amount of CO adsorption on $PdCl_2/Al_2O_3$ is 11.16 cm^3/g (STP) when the CO pressure approaches zero. Based on the BET surface area of monolayer $PdCl_2/Al_2O_3$ (174 m^2/g) and the impregnation loading of $PdCl_2$ on $PdCl_2/Al_2O_3$ (8.16×10^{-6} mol/m^2), we obtain the result that 1.0 mol of $PdCl_2$ adsorbs 0.35 mol of CO. That means that each molecule of $PdCl_2$ can adsorb 0.35 molecule of CO. This adsorption ratio of CO on $PdCl_2$ is similar to the result of Tamon et al. who reported that one molecule of $PdCl_2$ can adsorb around 0.4 molecule of CO at 50 °C.[27] The adsorption isotherms of CO on $PdCl_2$/AC and AC are shown in Figure 2. When the equilibrium pressure was extrapolated to zero, the saturation amounts of CO adsorption on $PdCl_2$/AC and AC are 7.82 and 0 cm^3/g (STP), respectively. This indicates that the adsorption of CO on AC is physical adsorption. Thus, the adsorbed amount of CO on $PdCl_2$/AC, 7.82 cm^3/g, can be assumed as the chemisorption amount of CO on $PdCl_2$ (i.e., the Benson-Boudart method). With the $PdCl_2$ loading of 19.7 wt% or 1.11×10^{-3} mol/g in $PdCl_2$/AC and the adsorption ratio of CO to $PdCl_2$ (0.35 mol/mol), the dispersion of $PdCl_2$ on AC was 89.4%. For the $PdCl_2$/AC sorbent, one may assume that the Cl^- ions from the $PdCl_2$

form a close-packed layer on the surface of AC and the Pd^{2+} ions occupy the interstices formed by Cl^-.[30] By taking 1.8 Å for the radius of Cl^- ion, it can be shown that 121 m^2 of the $PdCl_2$/AC surface area is covered by $PdCl_2$. This indicates that only 17.4% of $PdCl_2$/AC surface area (696 m^2/g) is covered by $PdCl_2$ or 82.6% of $PdCl_2$/AC surface area, 575 m^2/g, is bare surface of the activated carbon support.

The pore size distributions for various samples were measured by N_2 adsorption at 77K via the Horvath-Kawazoe (H-K) method.[32] Figure 3 shows the pore size distributions of monolayer $PdCl_2/Al_2O_3$ and Al_2O_3, and Figure 4 shows the pore size distributions of $PdCl_2$/AC and activated carbon support. As discussed elsewhere,[32] the original H-K model underestimates the total interaction energy of the adsorbate molecules, and after correction, the pore sizes are shifted toward higher (and correct) values.[32] After impregnation, the pores sizes were still large enough for the sulfur molecules to adsorb.

3.2 Fixed-bed adsorption experiment

After *in situ* activation of the adsorbent and wetting by *n*-octane, the model jet fuel (150 ppmw-S benzothiophene, 250 ppmw-S 2-methylbenzothiophene in 19.7 wt% benzene, 80 wt% *n*-octane containing 700 ppmw naphthalene) was allowed to contact the bed and the effluent benzothiophene (BT) sulfur and 2-methylbenzothiophene (MBT) sulfur contents were monitored periodically. Sulfur breakthrough (or elution) curves were generated by plotting the transient BT sulfur, MBT sulfur and total sulfur concentration normalized by the feed, versus cumulative fuel volume normalized by total bed weight. The sulfur adsorption amounts (normalized by adsorbent weight) were obtained after integrating of the area above the breakthrough curves. Table 3 summarizes the results

obtained for BT sulfur, MBT sulfur and total sulfur breakthrough and saturation adsorption amounts for the fresh sorbents.

Figure 5 shows the BT sulfur and MBT sulfur breakthrough curves obtained during treatment of the model jet fuel with the fresh CuCl/AC. The sorbent was capable of removing 0.048 and 0.070 mmol of BT sulfur per gram at breakthrough and saturation, respectively, while the sorbent was capable of removing 0.086 and 0.143 mmol of MBT sulfur per gram at breakthrough and saturation, respectively (Table 3). This result shows that the CuCl/AC sorbent had selectivity toward heavier, substituted benzothiophene over the nonsubstituted one. Based on molecular orbital calculations, Yang et al. showed that the methyl groups in the substituted thiophene compounds enhanced the electron back-donation process during π-complexation and, thus, resulted in higher energies of adsorption.[34] This agrees well with the profiles shown in Figure 5. However, the sulfur capacity was clearly equilibrium limited, i.e., the saturated sorbent was in equilibrium with the feed solution. The higher sulfur content for the MBT also resulted in higher sulfur capacities.

Figure 6 shows the results of desulfurization of the model jet fuel over the $PdCl_2$/AC sorbent. The results show that the $PdCl_2$/AC sorbent can remove 0.069 and 0.091 mmol of BT sulfur per gram at breakthrough and saturation, respectively, while the sorbent was capable of removing 0.126 and 0.187 mmol of MBT sulfur per gram at breakthrough and saturation for the same model jet fuel, respectively (Table 3). From the above results, it is seen that the $PdCl_2$/AC sorbent had higher sulfur capacity than that of CuCl/AC sorbent. Note that the amount of $PdCl_2$ salt, 1.11 mmol/g, on the activated carbon was similar to that of CuCl, 1.26 mmol/g, on activated carbon (Table 1). Because the pure AC had a

lower sulfur capacity than $PdCl_2$/AC in desulfruization of the model jet fuel (Table 3), it is concluded that the metal salt $PdCl_2$ contributed significantly by π-complexation toward adsorption of the sulfur-containing compounds. For 1 g of $PdCl_2$/AC, it took more than 20 min for the BT molecules to break through the adsorbent at a feed of 1.0 ml/10 min. Saturation was reached after 30 min.

To compare the adsorption ability of the metallic Pd for sulfur-containing compounds with that of Pd^{2+} (both are capable of π-complexation), a Pd/AC sorbent was tested for the desulfurization of the model jet fuel, as shown in Figure 7. The amounts of breakthrough and saturation were, respectively, 0.038 and 0.049 mmol/g for BT sulfur, 0.063 and 0.092 mmol/g for MBT sulfur. From the breakthrough curves, the $PdCl_2$/AC sorbent adsorbed almost twice as much compared with Pd/AC, showing that the interactions were stronger between Pd^{2+} and organosulfur than that between Pd metal and organosulfur.

Figure 8 shows the BT sulfur and MBT sulfur breakthrough curves obtained for desulfurization of the model jet fuel with fresh activated carbon support. The pure carbon support was capable of removing 0.110 and 0.176 mmol of total sulfur per gram at breakthrough and saturation, respectively (Table 3). This result shows that the activated carbon support played an important role in the desulfurization of the model jet fuel.

Figure 9 shows the breakthrough adsorption of the total organosulfur molecules in desulfurization of the model jet fuel with three carbon-based adsorbents, Pd/AC, CuCl/AC and $PdCl_2$/AC. It is clear that all of the sorbents were capable of removing BT and MBT molecules. For the same feed described above, $PdCl_2$/AC showed the highest capacities among the adsorbents studied. The breakthrough and saturation capacities for

total sulfur were 0.184 and 0.278 mmol/g, indicating strong interactions with BT and MBT molecules. For about 1 g of $PdCl_2$/AC, it can treat about 20 ml of the model jet fuel to less than 1 ppmw-S.

To compare the sulfur capacities of $PdCl_2$ on different supports, desulfurization by $PdCl_2/Al_2O_3$ was also tested under the same feed conditions, shown in Figure 10. It is clear that the sulfur capacity of $PdCl_2$/AC with the model jet fuel was higher than that of $PdCl_2/Al_2O_3$. From these results, activated carbon was a more effective support than Al_2O_3 for the $PdCl_2$ supported sorbents for desulfurization of fuel containing benzothiophene and substituted compounds.

Based on the results above, the normalized selective sulfur adsorption capacities of the $PdCl_2$ surface and that of the activated carbon surface can be calculated. Since the fraction of the surface area of the $PdCl_2$/AC sorbent that is covered by $PdCl_2$ is already known (see "Characterization"), it is possible to predict the sulfur capacity of supported $PdCl_2$/AC sorbent, by taking the weighted average. The normalized adsorption capacity of $PdCl_2$ was obtained from the monolayer $PdCl_2/Al_2O_3$ sorbent where the surface was compeletly covered by the $PdCl_2$ salt. The normalized sulfur capacities per m^2, both at the breakthrough point and at saturation, are listed in Table 4. Combining the normalized adsorption capacity of $PdCl_2$ and activated carbon as well as the surface areas of the $PdCl_2$/AC sorbent (i.e., 676 m^2/g), the bare carbon (575 m^2/g) and the $PdCl_2$ (121 m^2/g) on $PdCl_2$/AC, the predicted adsorption capacity of $PdCl_2$/AC can be calculated. The calculation results showed that 18.3×10^{-5} and 29.8×10^{-5} mmol of total sulfur per m^2 at breakthrough and saturation, respectively, can be adsorbed by of $PdCl_2$/AC sorbent. However, the experimental results showed that the normalized total sulfur capacities were

26.4×10^{-5} and 40.0×10^{-5} mmol/m^2 at breakthrough and saturation, respectively (Table 4). Thus, the experimental results are substantially higher than the predicted results based on weighted average. The difference between experiment and calculation results shows that an additional factor affects the adsorption capacity of $PdCl_2$/AC sorbent during the desulfurization of model fuel. Clearly, there was a synergistic effect between the carbon substrate and the supported metal salt that caused the significantly enhanced sulfur capacity.

For π-complexation sorbents, the charge-compensating anion has a very strong effect on the π-complexation by the cation.[32] The effects of the substrate on the metal salt, if any, are much weaker. Thus, any electronic effect as the reason for the strong synergistic effect discussed above is ruled out. One would resort to a geometric effect as a possible explanation. Since the $PdCl_2$ salt was well spread on the carbon substrate, there existed a large number of peripheral sites on the edges of the supported metal salt. These edge sites provided an ideal combination of sites for the benzothiophene molecule: $PdCl_2$ for the thiophene ring and carbon for the benzene ring. Adsorption of a substituted methylbenzothiophene molecule on such an edge site is depicted in Figure 11. In this depiction, benzene ring is adsorbed strongly on the surface of carbon, while the thiophene ring is bonded to the Pd^{2+} by π-complexation.

From the above results, it can be seen that $PdCl_2$/AC is the best sorbent for desulfurization of the model jet fuel among all of the tested carbon-based sorbents. As predicted by our molecular order calculations,[28,34] the metal ion Pd^{2+} is stronger for π-complexation than Cu^+ and Pd^0. Furthermore, it is shown in this work that activated carbon is a most effective support for π-complexation sorbents.

A comparison between the two π-complexation sorbents, $PdCl_2$/AC and Cu(I)Y zeolite, is in order. For a similar model jet fuel, our results showed that the Cu(I)Y (vapor-phase ion exchanged) was significantly better, because it could produce about 30 ml/g clean fuel (< 1 ppmw S) at the breakthrough point, compared with ~22 ml/g for $PdCl_2$/AC.[28] However, the $PdCl_2$/AC sorbent was much better for the commercial JP-5 jet fuel (with 1172 ppmw S).[28] The apparent reason for these results is that, for $PdCl_2$/AC, the large aromatic compounds (e.g., polynuclear aromatics and organo-nitrogen compounds) in the commercial jet fuel were adsorbed on the bare surfaces of the activated carbon support and were not competing for the Pd^{2+} sites, which were used for bonding with the benzothiophenes.

An important note on the desulfurization capability (or the lack of) of the (undoped) activated carbon is in order. As shown in Figure 8, activated carbon seems to have good sulfur selectivity and capacity for the "model" fuel. Similar results were also shown by others for other "model" fuels.[4,23] However, when "real" commercial fuels were used, very early breakthrough of sulfur would appear from the fixed-bed adsorber. This was shown in our earlier work for a commercial diesel.[1] To show a direct comparison, we performed the breakthrough curves for the activated carbon and that with $PdCl_2$ dopant ($PdCl_2$/AC), using the same commercial JP-5 fuel (with 1172 ppmw-S). Details of the JP-5 fuel have been reported elsewhere.[28] Figure 12 shows the results for desulfurization of JP-5 with $PdCl_2$/AC and pure activated carbon. The results show clearly that the π-complexation sorbent ($PdCl_2$) has the high sulfur selectivity that the activated carbon lacks. Similar results have been reported for a commercial fuel with Cu(I)Y and

activated.[1] The advantage for using the π-complexation sorbents is clearly seen by these comparisons.

3.3 Sorbent regeneration

The $PdCl_2$/AC sorbent was tested for regeneration after saturation with the model jet fuel. The regeneration was conducted by desorption in a static bath of solvent. The $PdCl_2$/AC sorbent was first saturated with the model jet fuel. Then the saturated sorbent was regenerated at room temperature and 50ºC. Figure 13 shows the results of desorption in a mixture of 30 wt% benzene and 70 wt% *n*-octane. The amount of sulfur desorbed depended on the time and temperature. With increasing regeneration time, the amount of sulfur desorbed reached a constant value. Therefore, it could be expected that substantially more sulfur could be desorbed at a higher temperature with adequate time. Figure 13 showed that approximately 35 wt% and 45 wt% of the total sulfur in the sorbent were desorbed, respectively, at room temperature and 50ºC, after 30 min.

In our previous study,[2] it was found that ultrasound was an effective technique for regenerating spent $CuCl/Al_2O_3$ sorbent at room temperature. In this work, the ultrasound technique was also applied to regenerate the spent $PdCl_2$/AC sorbent. Figure 14 shows the results of desorption with ultrasound and without ultrasound, both at 50 ºC. The amount of sulfur desorbed was higher with ultrasound, 65 wt% desorption vs. 45 wt% desorption without ultrasound. This result indicates that the saturated $PdCl_2$/AC sorbent could be effective regenerated by the ultrasound technique.

4. Conclusion

Several carbon-base sorbents were investigated for desulfurization of a model jet fuel (150 ppmw-S BT and 250 ppmw-S MBT in 19.75 wt% benzene + 80 wt% *n*-octane

containing 700 ppmw naphthalene). The results showed that the selective adsorption ability of $PdCl_2$ was higher than CuCl and metallic Pd. It was also found that activated carbon was the best support for supported $PdCl_2$ adsorbents to remove sulfur-containing compounds, i.e. benzothiophene and methlybenzothiophene. Among all tested adsorbents in this work, $PdCl_2$/AC had the highest capacity to remove sulfur-containing compounds from the model jet fuel. A significant synergistic effect was observed between the carbon substrate and the supported π-complexation sorbent, and this effect was explained by a geometric effect.

The results of regeneration experiments showed that ultrasound-assisted regeneraton was a effective method for the saturated $PdCl_2$/AC that was saturated with benzothiophene and substituted compounds. The amount of sulfur desorbed was higher with ultrasound, 65 wt% desorption vs. 45 wt% without ultrasound.

References

(1) Hernández-Maldonado, A. J.; Yang, R. T. *Catal. Rev.* **2004**, *46*, 111.

(2) Hernández-Maldonado, A. J.; Qi, G. S.; Yang, R.T. *Appl. Catal. B* **2005**, *61*, 212.

(3) Kemsley, J. *Chem. Eng. News* **2003**, *81*, 40.

(4) Haji, S.; Erkey, C. *Ind. Eng. Chem. Res.* **2003**, *42*, 6933.

(5) McKinley, S. G.; Angelici, R. J. *Chem. Commun.* 2003, 2620.

(6) Ng, F. T. T.; Rahman, A.; Ohasi, T.; Jiang, M. *Appl. Catal. B*. **2005**, *56*, 127.

(7) Yang, X. X.; Erickson, L. E.; Hohn, K. L.; Jeevanandam, P.; Klabunde, K. J. *Ind. Eng. Chem. Res.* **2006**, *45*, 6169.

(8) Jeevanandam, P.; Klabunde, K. J.; Tetzler, S. H. *Micropor. Mesopor. Mater.* **2005**, *79*, 101.

(9) Jiang, M.; Ng, F. T. T. *Catal. Today* **2006**, *116*, 530.

(10) Yang, R. T.; Hernández-Maldonado, A. J.; Yang, F. H. *Science* **2003**, *301*, 79.

(11) Yang, R. T.; Takahashi, A.; Yang, F. H.; Hernández-Maldonado, A. J. U.S. and Foreign Patent Applications Filed, **2002**.

(12) Hernández-Maldonado, A. J.; Yang, R. T. J. *Am. Chem. Soc.* **2004**, *126*, 992.

(13) Hernández-Maldonado, A. J.; Yang, R. T. *AIChE J.* **2004**, *50*, 791.

(14) Hernández-Maldonado, A. J.; Yang, R. T. *Angew. Chem. Int. Edit.* **2004**, *43*, 1004.

(15) Hernández-Maldonado, A. J.; Stamatis, S. D.; Yang, R. T.; He, A. Z.; *Ind. Eng. Chem. Res.* **2004**, *43*, 769.

(16) Hernández-Maldonado, A. J.; Yang, F. H.; Qi, G.; Yang, R. T. *Appl. Catal. B.* **2005**, *56*, 111.

(17) Takahashi, A.; Yang, R. T.; Muncon, C. L.; Chin, D. *Langmuir* **2001**, *17*, 8405.

(18) Ma, X.; Velu, S.; Kim, J.H.; Song, C. *Appl. Catal. B* **2005**, *56*, 137.

(19) King, D. L.; Li, L.Y. *Catal. Today* **2006**, *116*, 526.

(20) Hernández-Maldonado, A. J.; Yang, R. T. *Ind. Eng. Chem. Res.* **2003**, *42*, 3103.

(21) Sano, Y.; Choi, K. H.; Korai, Y.; Mochida, I. *Energy & Fuels* **2004**, *18*, 644.

(22) Jiang, Z.; Liu, Y.; Sun, X.; Tian, F.; Sun, F., Liang, C.; You, W.; Han, C.; Li, C. *Langmuir* **2003**, *19*, 731.

(23) Zhou, A. N.; Ma, X. L.; Song, C. S. *J. Phys. Chem. B* **2006**, *110*, 4699.

(24) Kim, J. H.; Ma, X. L.; Zhou, A. N.; Song, C. S. *Catal. Today* **2006**, *111*, 74.

(25) Sano, Y.; Choi, K. H.; Korai, Y.; Mochida, I. *Appl. Catal. B* **2004**, *49*, 219.

(26) Lee, S. H. D.; Kumar R.; Krumpelt. R. *Sep. Purif. Technol.* **2002**, *26*, 247.

(27) Tamon, H.; Kitamura, K.; Okazaki. M. *AIChE J.* **1996**, *42*, 422.

(28) Wang, Y. H.; Yang, F. H.; Yang, R. T.; Heinzel, J, M.; Nickens, A. D. *Ind. Eng. Chem. Res*., **2006**, *45,* 7649.

(29) Amorim, C.; Yuan, G.; Patterson, P. M.; Keane, M. A. *J. Catal*. **2005**, *234*, 268.

(30) Xie, Y. C.; Tang, Y. Q. *Adv*. *Catal*. **1990**, *37*, 1.

(31) Velu, S.; Ma, X. L.; Song. C. S. *Ind*. *Eng*. *Chem*. *Res*. **2003**, *42*, 5293.

(32) Yang, R. T., *Adsorbents: Fundamentals and Applications,* Wiley, New York, 2003.

(33) Schueller. B. S.; Yang, R.T. *Ind. Eng*. *Chem*. *Res*. **2001**, *40*, 4912.

(34) Yang, F. H.; Hernández-Maldonado, A. J.; Yang. R.T. *Separ. Sci. Technol*. **2004**, *39*, 1717.

Table 1 Characterization of sorbents

Sorbent	Loading of metal salt (wt%)	Content of metal element (mmol/g)	BET surface area (m^2/g)
AC	-	-	998
Pd/AC	30.1 [$Pd(NO_3)_2$]	1.31	561
$PdCl_2$/AC	19.7 [$PdCl_2$]	1.11	696
CuCl/AC	12.5 [CuCl]	1.26	864
Al_2O_3	-	-	340
$PdCl_2/Al_2O_3$	33.3 [$PdCl_2$]	1.88	174

Table 2 Composition of model jet fuel used in present work

Compound	F.W. (g/mol)	Content of compound (wt%)	Content of S (ppmw)	Concentration of compound (mmol/l)
Benzothiophene	134.20	0.063	150.0	3.45
2-methybenzothiophene	148.23	0.116	250.0	5.75
Naphthalene	128.17	0.071	-	4.07
Benzene	78.11	19.75	-	1856.4
n-octane	114.23	80.0	-	5141.9

Table 3 Breakthrough and saturation loadings for BT, MBT and total sulfur from model jet fuel on different sorbents

Sorbent	Breakthrough loading (mmol/g)			Saturation loading (mmol/g)		
	BT	MBT	Total	BT	MBT	Total
AC	0.041	0.069	0.110	0.056	0.120	0.176
CuCl/AC	0.048	0.086	0.128	0.070	0.143	0.212
$PdCl_2$/AC	0.069	0.126	0.184	0.091	0.187	0.278
Pd/AC	0.038	0.063	0.101	0.049	0.092	0.142
$PdCl_2/Al_2O_3$	0.034	0.063	0.092	0.052	0.101	0.153

Table 4 Normalized adsorption capacity of sorbents for BT, MBT and total sulfur from model jet fuel at breakthrough and saturation

Sorbent	Breakthrough loading ($mmol/10^5\ m^2$)			Saturation loading ($mmol/10^5\ m^2$)		
	BT	MBT	Total	BT	MBT	Total
AC	4.1	6.9	11.0	5.6	12.0	17.6
CuCl/AC	5.6	10.0	14.8	8.1	16.6	24.5
$PdCl_2$/AC	10.0	18.1	26.4	13.1	26.9	40.0
Pd/AC	6.8	11.2	18.0	8.7	16.4	25.3
$PdCl_2/Al_2O_3$	21.8	36.2	52.9	36.2	58.0	87.9

Figure Captions

Fig. 1 Equilibrium isotherm of CO on monolayer $PdCl_2/\gamma\text{-}Al_2O_3$ at 35 °C.

Fig. 2 Equilibrium isotherm of CO on $PdCl_2$/AC (■) and AC (●) at 35 °C.

Fig. 3 H-K differential pore volume distribution of $\gamma\text{-}Al_2O_3$ (⋯) and monolayer $PdCl_2/\gamma\text{-}Al_2O_3$ (—).

Fig. 4 H-K differential pore volume distribution of activated carbon (—) and $PdCl_2$/AC (⋯).

Fig. 5 Breakthrough of BT and MBT sulfur in a fixed-bed adsorber with CuCl/AC (1.0 g), for model fuel (150 ppmw-S BT and 250 ppmw-S MBT in 19.75 wt% benzene + 80 wt% *n*-octane containing 700 ppmw naphthalene) at room temperature. Ci is the total sulfur concentration of the feed at flow rate 1.0 ml/10 min (S.V. = 4.6 h^{-1}).

Fig. 6 Breakthrough of BT and MBT sulfur in a fixed-bed adsorber with $PdCl_2$/AC (1.0 g), for model fuel (150 ppmw-S BT and 250 ppmw-S MBT in 19.75 wt% benzene + 80 wt% *n*-octane containing 700 ppmw naphthalene) at room temperature. Ci is the total sulfur concentration of the feed at flow rate 1.0 ml/10 min (S.V. = 4.6 h^{-1}).

Fig. 7 Breakthrough of BT and MBT sulfur in a fixed-bed adsorber with Pd/AC (1.0 g), for model fuel (150 ppmw-S BT and 250 ppmw-S MBT in 19.75 wt% benzene + 80 wt% *n*-octane containing 700 ppmw naphthalene) at room temperature. Ci is the total sulfur concentration of the feed at flow rate 1.0 ml/10 min (S.V. = 5.5 h^{-1}).

Fig. 8 Breakthrough of BT and MBT sulfur in a fixed-bed adsorber with AC (1.0 g, Type PCB,), for model fuel (150 ppmw-S BT and 250 ppmw-S MBT in 19.75 wt% benzene + 80 wt% *n*-octane containing 700 ppmw naphthalene) at room temperature. Ci is the total sulfur concentration of the feed at flow rate 1.0 ml/10 min (S.V. = 3.1 h^{-1}).

Fig. 9 Breakthrough of total sulfur in a fixed-bed adsorber with Pd/AC (●), CuCl/AC (□) and $PdCl_2$/AC (○), for model fuel (150 ppmw-S BT and 250 ppmw-S MBT in 19.75 wt% benzene + 80 wt% *n*-octane containing 700 ppmw naphthalene) at room temperature. Ci is the total sulfur concentration of the feed at flow rate 1.0 ml/10 min.

Fig. 10 Breakthrough of total sulfur in a fixed-bed adsorber with monolayer $PdCl_2$/γ-Al_2O_3 (●) and $PdCl_2$/AC (○), for Model fuel (150 ppmw-S BT and 250 ppmw-S MBT in 19.75 wt% benzene + 80 wt% *n*-octane containing 700 ppmw naphthalene) at room temperature. Ci is the total sulfur concentration of the feed at flow rate 1.0 ml/10 min (S.V. = 4.6 h^{-1}) for $PdCl_2$/AC and 1 cm^3/20 min (S.V. = 3.4 h^{-1}) for $PdCl_2$//γ-Al_2O_3.

Fig. 11 Depiction of synergistic effect in adsorption of methylbenzothiophene on $PdCl_2$/AC.

Fig. 12 Breakthrough of total sulfur in a fixed-bed adsorber with pure AC (■) and $PdCl_2$/AC (●), for JP-5 Jet fuel (1172 ppmw-S) at room temperature. Ci is the total sulfur concentration of the feed at flow rate 1 cm^3/20 min (S.V. = 2.3 h^{-1}).

Fig. 13 Amount of total sulfur desorbed (in percent, g-S/g-sorbent) from saturated $PdCl_2$/AC sorbent regenerated at 20 °C (○) and 50 °C (●) in a static system with 30 wt% benzene and 70 wt% *n*-octane.

Fig. 14 Amount of total sulfur desorbed (in percent, g-S/g-sorbent) from saturated $PdCl_2$/AC with ultrasound (□) and without ultrasound (■) at 50 °C in a static system with 30 wt% benzene and 70 wt% *n*-octane.

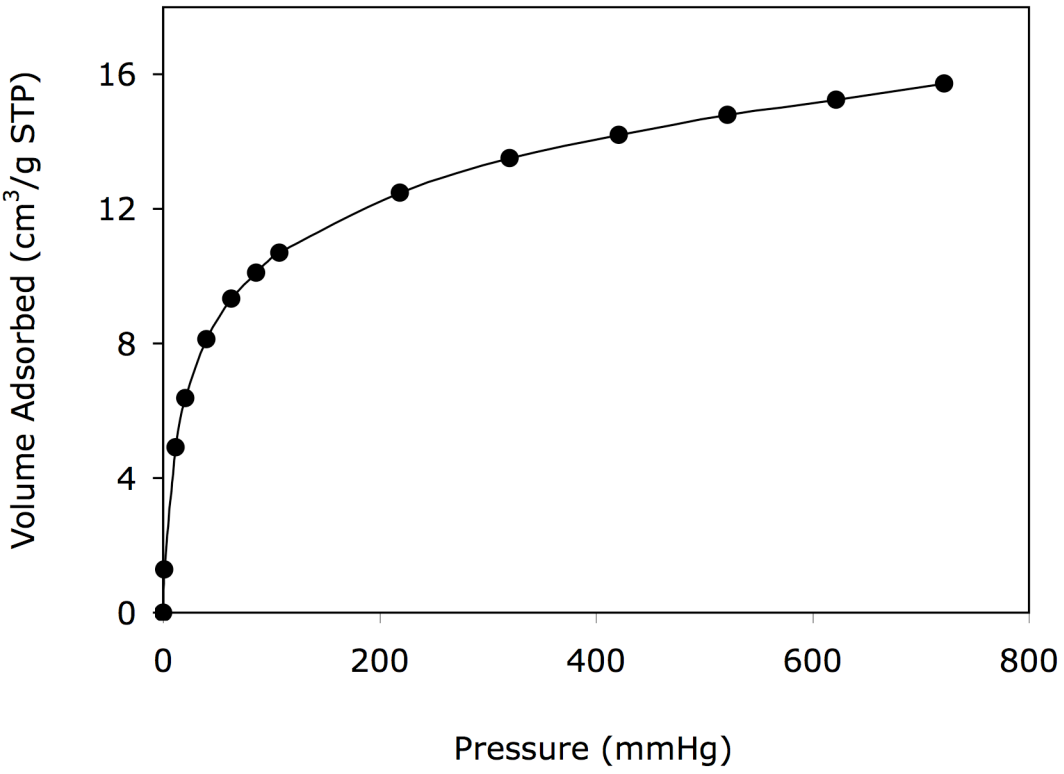

Fig. 1 Isotherm plot of CO on monolayer $PdCl_2/Al_2O_3$ at 35 ºC

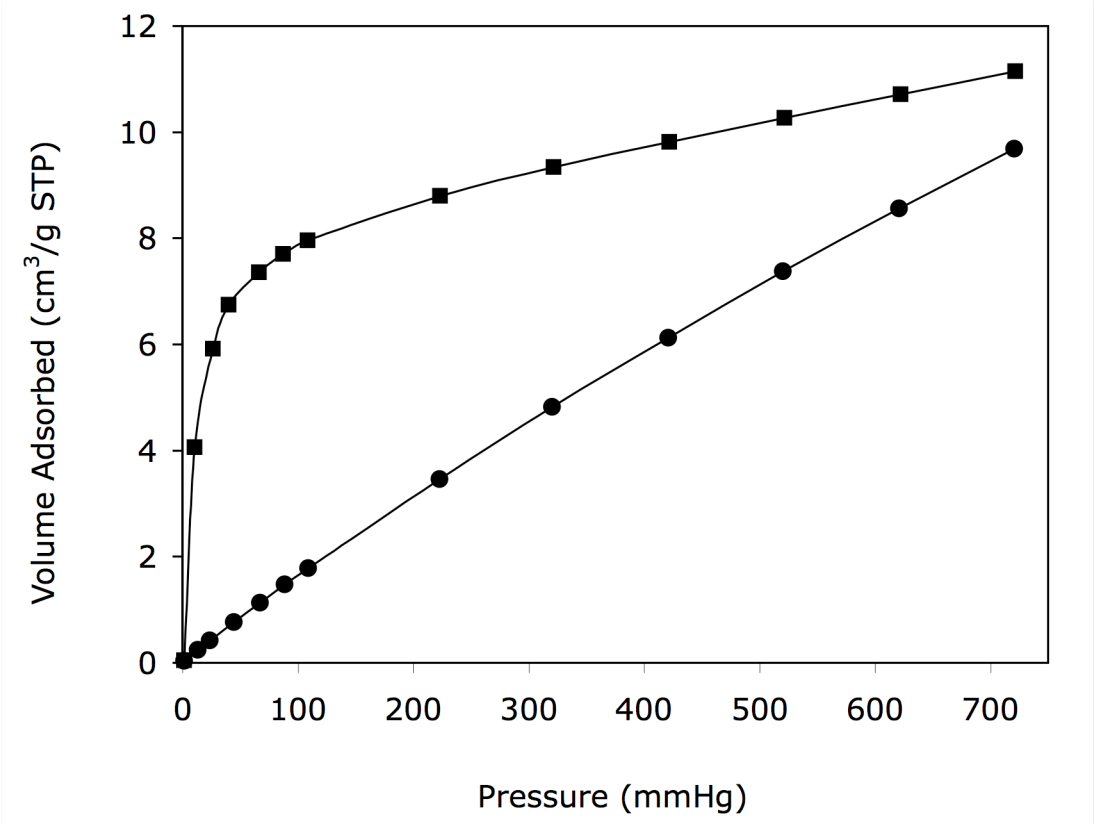

Fig. 2 Isotherm plot of CO on $PdCl_2$/AC (■) and AC (●) at 35 °C

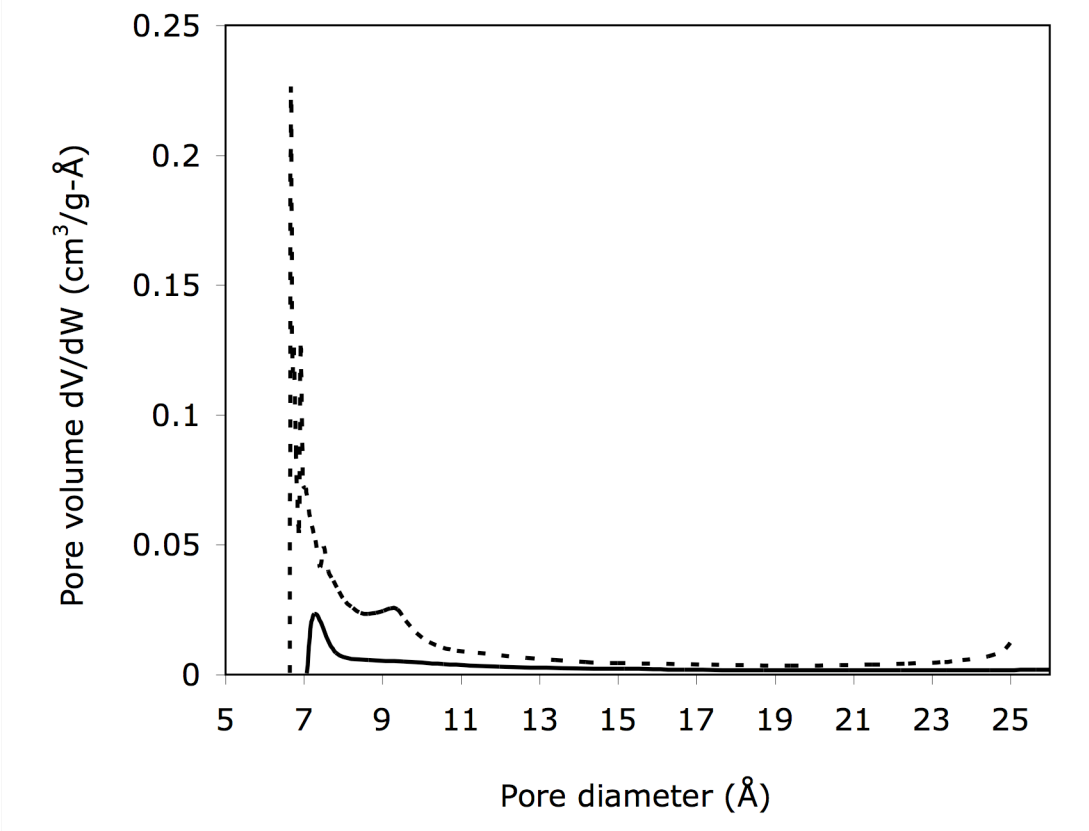

Fig. 3 H-K Differential pore volume plots of γ-Al_2O_3 (⋯) and monolayer $PdCl_2$/γ-Al_2O_3 (—).

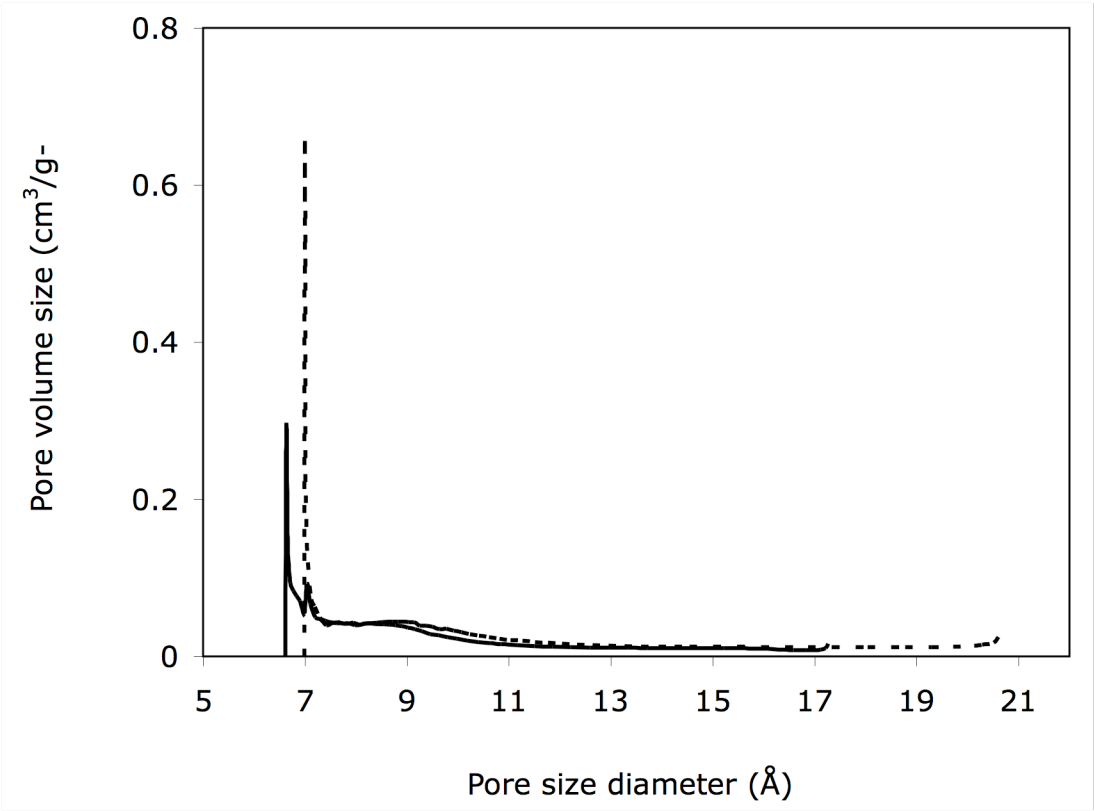

Fig. 4 H-K Differential pore volume plots of activated carbon (—) and $PdCl_2$/AC (⋯).

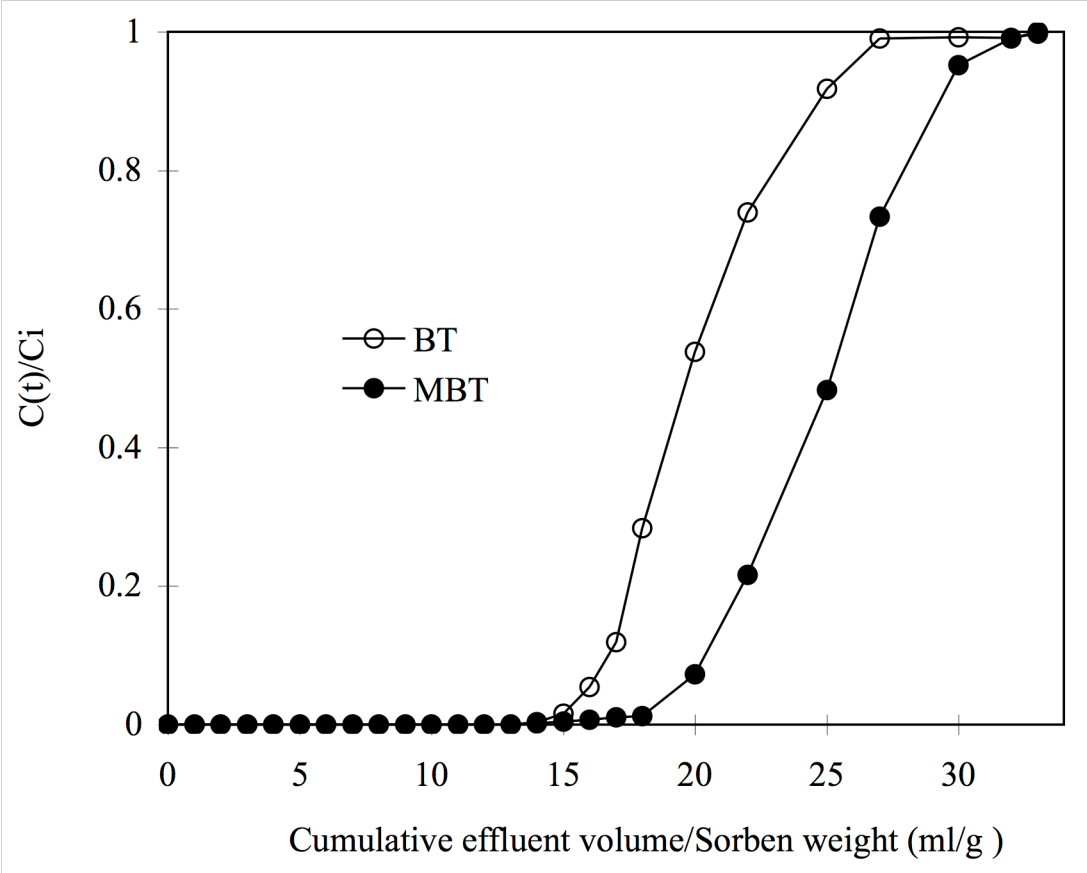

Fig. 5 Breakthrough of BT and MBT sulfur in a fixed-bed adsorber with CuCl/AC (1.0 g), for Model fuel (150 ppmw-S BT and 250 ppmw-S MBT in 19.75 wt% benzene + 80 wt% *n*-octane containing 700 ppmw naphthalene) at room temperature. Ci is the total sulfur concentration of the feed at flow rate 1.0 ml/10 min (S.V. = 4.6 h^{-1}).

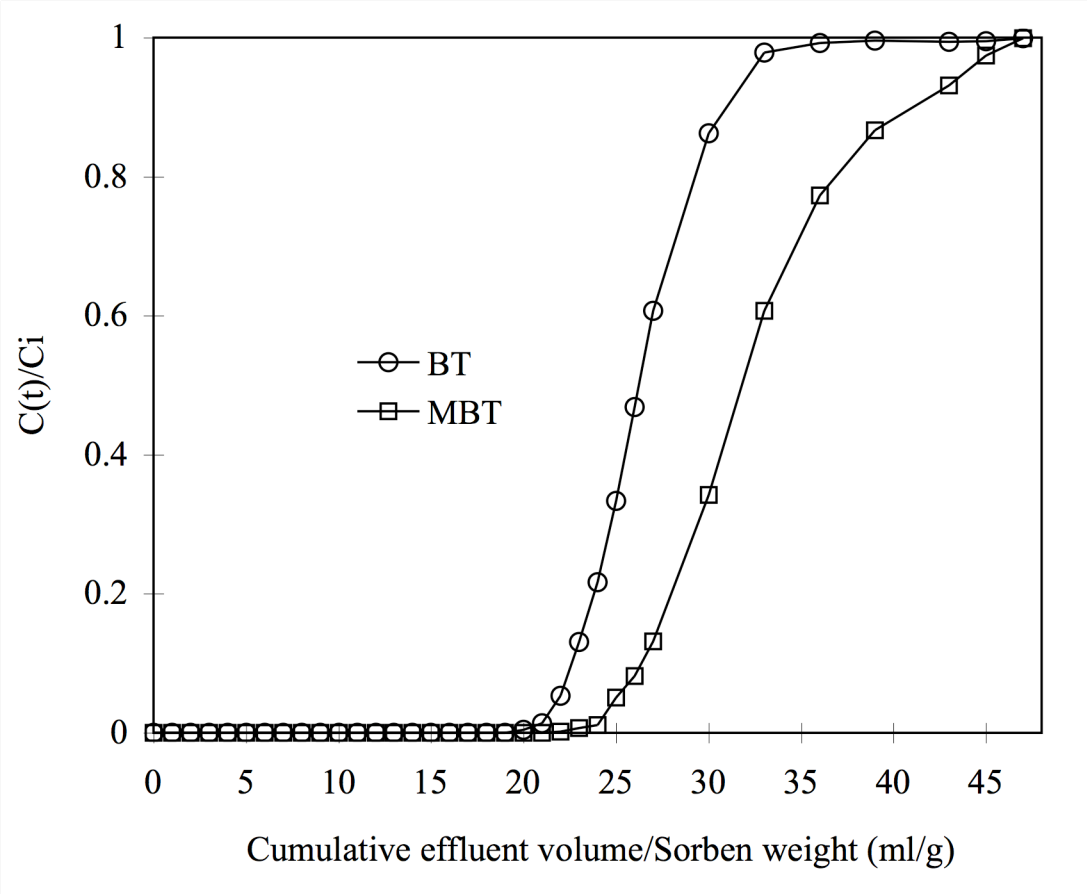

Fig. 6 Breakthrough of BT and MBT sulfur in a fixed-bed adsorber with $PdCl_2$/AC (1.0 g), for Model fuel (150 ppmw-S BT and 250 ppmw-S MBT in 19.75 wt% benzene + 80 wt% *n*-octane containing 700 ppmw naphthalene) at room temperature. Ci is the total sulfur concentration of the feed at flow rate 1.0 ml/10 min (S.V. = 4.6 h^{-1}).

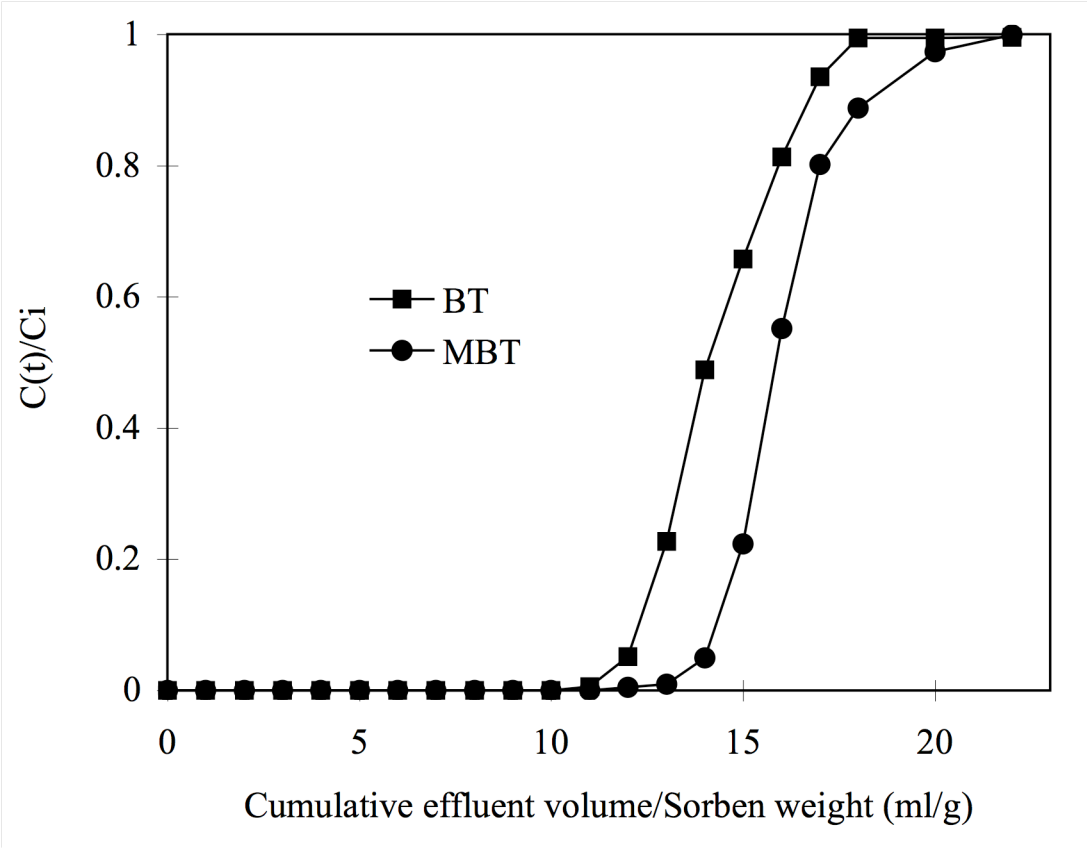

Fig. 7 Breakthrough of BT and MBT sulfur in a fixed-bed adsorber with Pd/AC (1.0 g), for Model fuel (150 ppmw-S BT and 250 ppmw-S MBT in 19.75 wt% benzene + 80 wt% *n*-octane containing 700 ppmw naphthalene) at room temperature. Ci is the total sulfur concentration of the feed at flow rate 1.0 ml/10 min (S.V. = 5.5 h^{-1}).

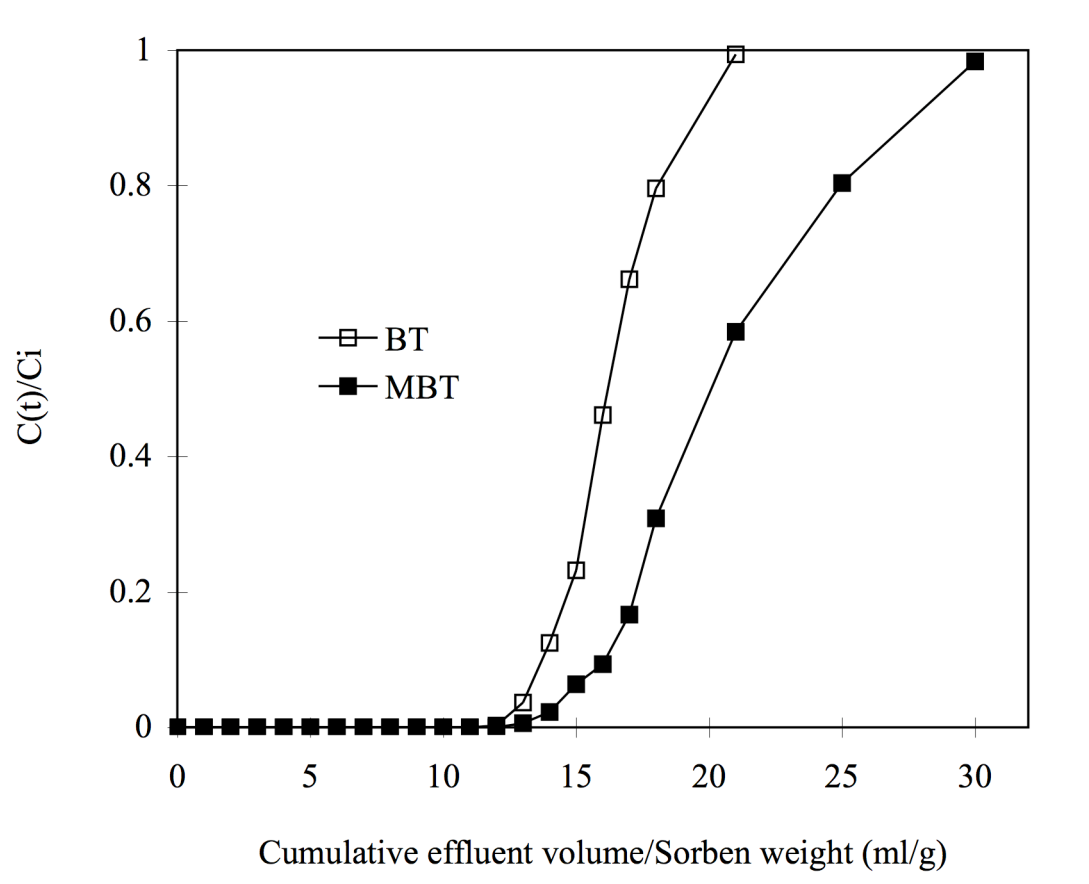

Fig. 8 Breakthrough of BT and MBT sulfur in a fixed-bed adsorber with AC (1.0 g, Type PCB,), for Model fuel (150 ppmw-S BT and 250 ppmw-S MBT in 19.75 wt% benzene + 80 wt% *n*-octane containing 700 ppmw naphthalene) at room temperature. Ci is the total sulfur concentration of the feed at flow rate 1.0 ml/10 min (S.V. = 3.1 h^{-1}).

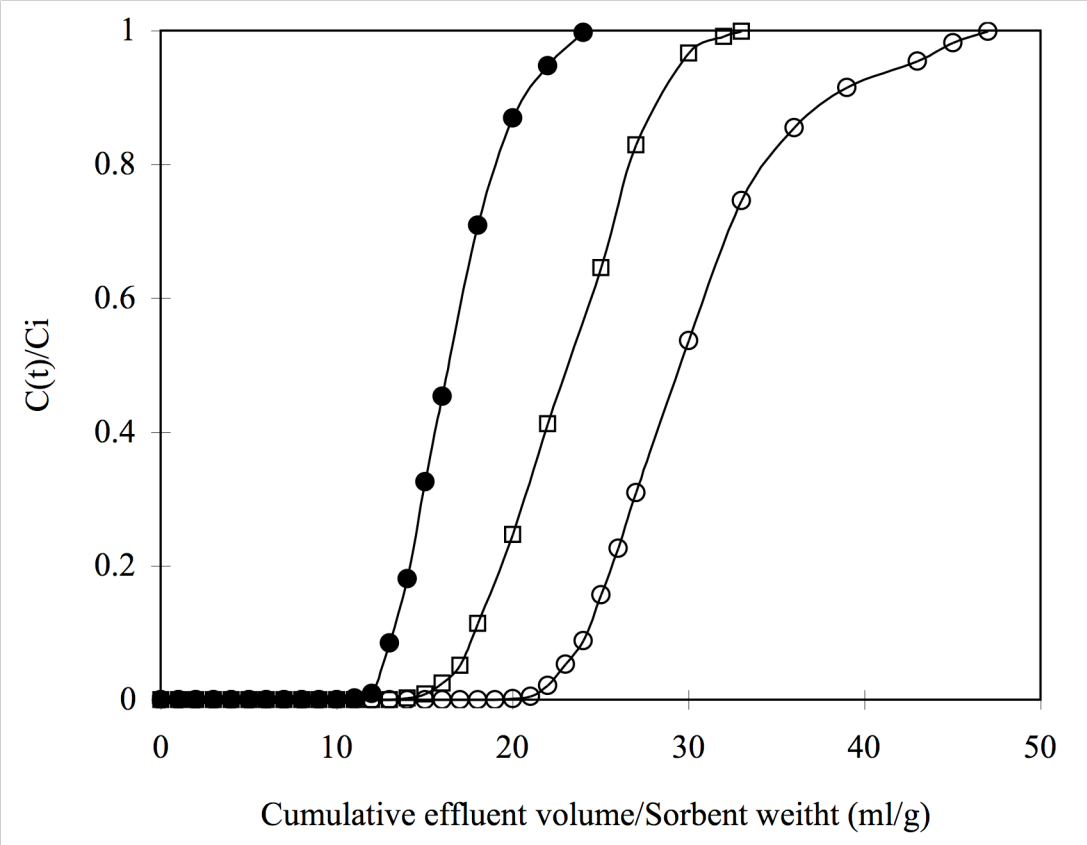

Fig. 9 Breakthrough of total sulfur in a fixed-bed adsorber with Pd/AC (●), CuCl/AC (□) and $PdCl_2$/AC (○), for Model fuel (150 ppmw-S BT and 250 ppmw-S MBT in 19.75 wt% benzene + 80 wt% *n*-octane containing 700 ppmw naphthalene) at room temperature. Ci is the total sulfur concentration of the feed at flow rate 1.0 ml/10 min.

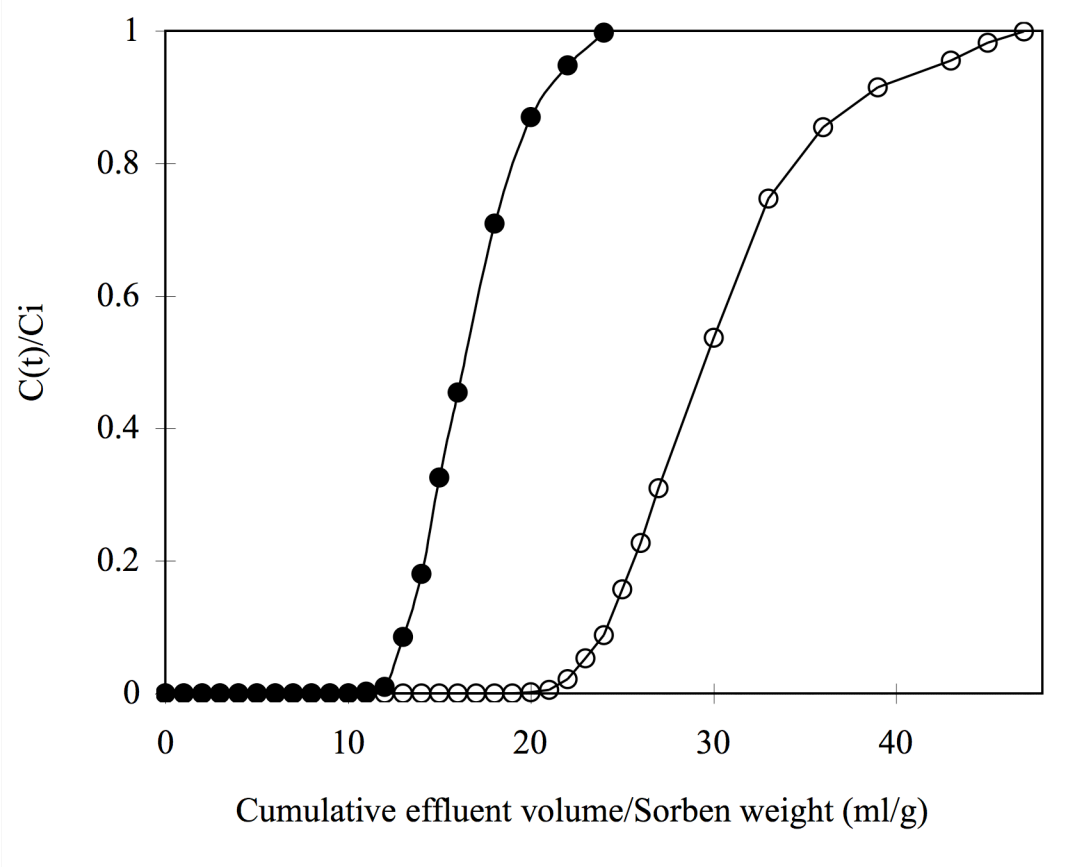

Fig. 10 Breakthrough of total sulfur in a fixed-bed adsorber with monolayer $PdCl_2/\gamma$-Al_2O_3 (●) and $PdCl_2$/AC (○), for Model fuel (150 ppmw-S BT and 250 ppmw-S MBT in 19.75 wt% benzene + 80 wt% *n*-octane containing 700 ppmw naphthalene) at room temperature. Ci is the total sulfur concentration of the feed at flow rate 1.0 ml/10 min (S.V. = 4.6 h^{-1}) for $PdCl_2$/AC and 1 cm^3/20 min (S.V. = 3.4 h^{-1}) for $PdCl_2$//γ-Al_2O_3.

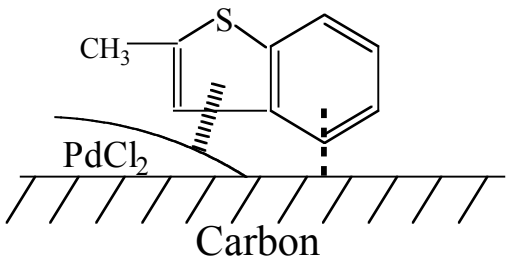

Fig. 11 Depiction of synergistic effect in adsorption of methylbenzothiophene on $PdCl_2$/AC.

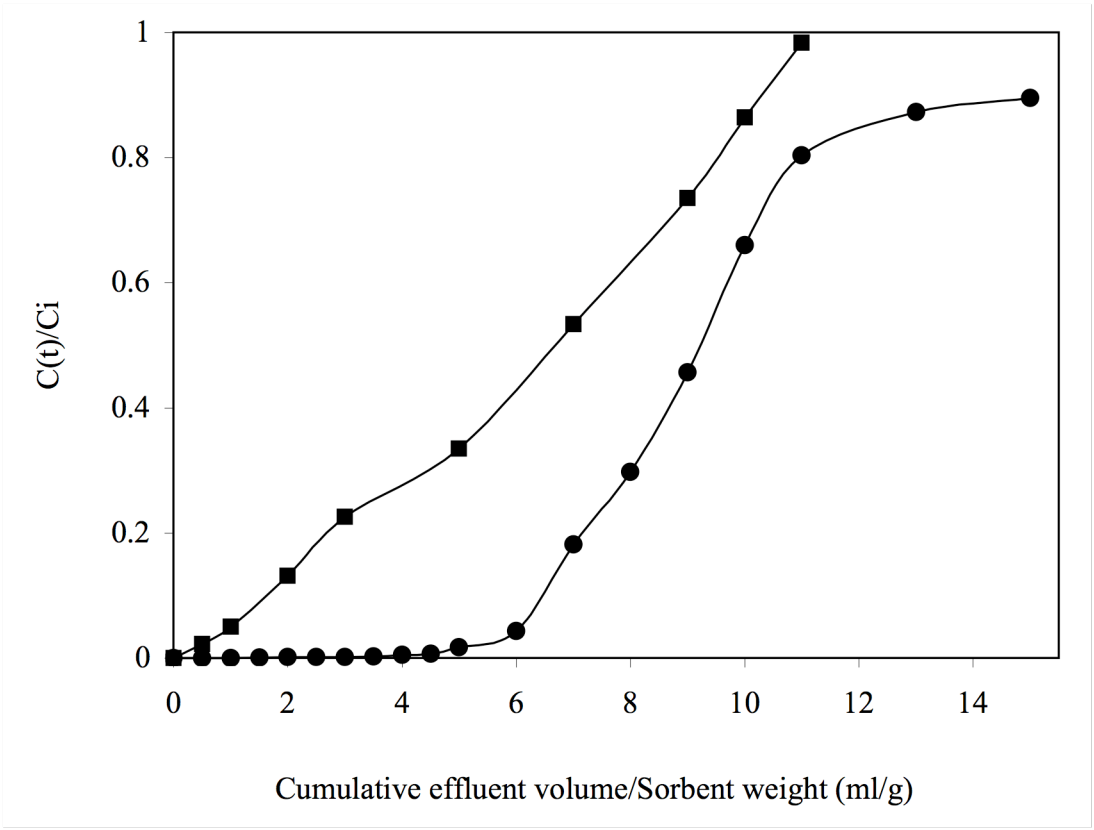

Fig. 12 Breakthrough of total sulfur in a fixed-bed adsorber with pure AC (■) and $PdCl_2$/AC (●), for JP-5 Jet fuel (1172 ppmw-S) at room temperature. Ci is the total sulfur concentration of the feed at flow rate 1 cm^3/20 min (S.V. = 2.3 h^{-1}).

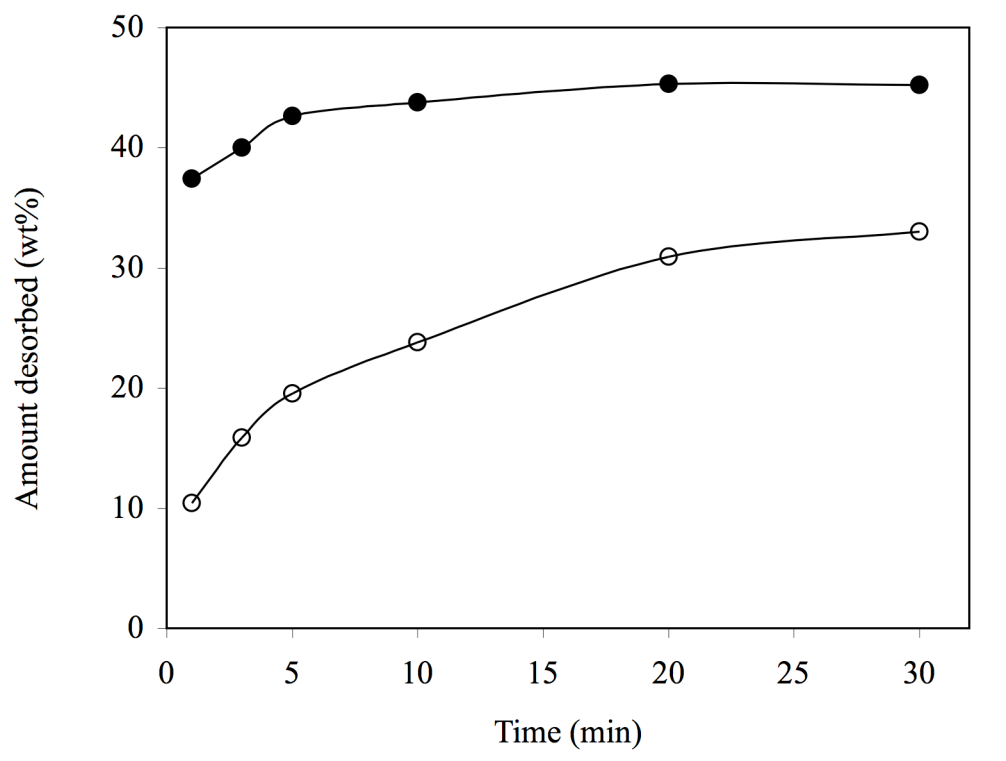

Fig. 13 Amount of total sulfur desorbed (in percent, g-S/g-sorbent) from spent $PdCl_2$/AC sorbent regenerated at 20 ºC (○) and 50 ºC (●) in a static system with 30 wt% benzene and 70 wt% *n*-octane.

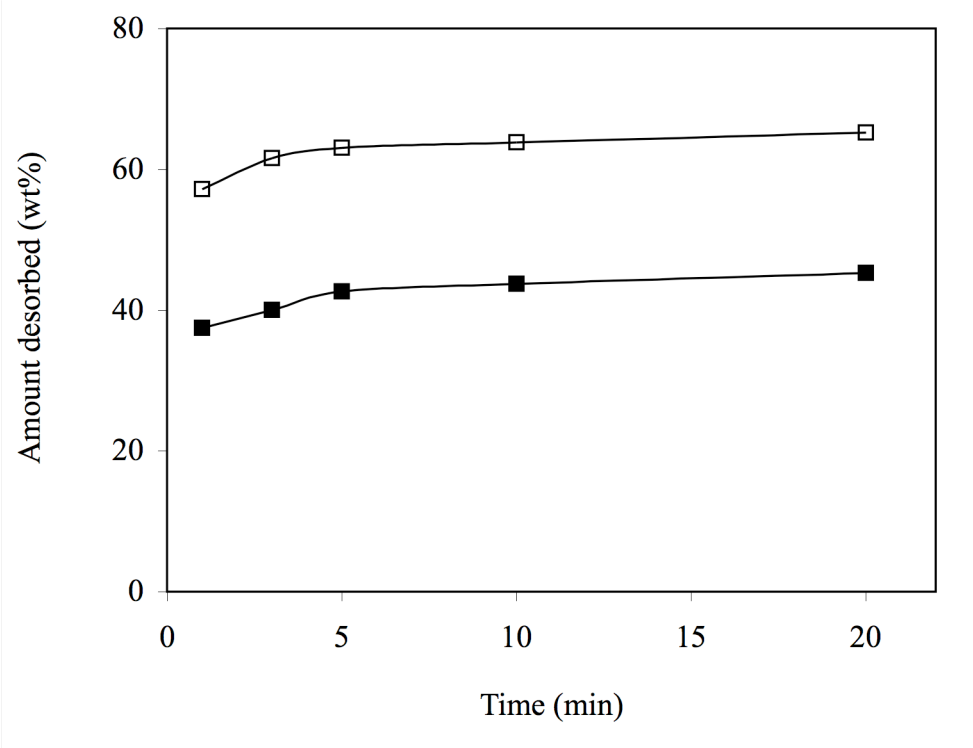

Fig. 14 Amount of total sulfur desorbed (in percent, g-S/g-sorbent) from spent $PdCl_2$/AC with ultrasound (□) and no ultrasound (■) at 50 ºC in a static system with 30 wt% benzene and 70 wt% *n*-octane.

Section 2: Selective Adsorption of Sulfur Compounds: Isotherms, Heats and Relationship between Adsorption from Vapor and Liquid Solution

1. Introduction

Deep desulfurization of transportation fuels (gasoline, diesel and jet fuels) is being mandated by U.S. and foreign governments, and is also needed for fuel cell applications.[1] A great deal of attention has been paid to developing new approaches to ultra deep desulfurization of liquid hydrocarbon fuels worldwide.[2-6] Selective adsorption is of particular interest. Various types of adsorbents such as mixed metal oxides, active carbon, clays, zeolites and some novel mesoporous materials have been studied.[6-14]

In our previous studies, we have developed a class of sorbents that rely on π-complexation for selective adsorption of organic sulfur molecules from liquid fuels.[15-21] These sorbents were prepared by using several ion-exchange techniques to introduce d-block metal cations into zeolites , including Ag^+, Cu^+, Ni^{2+}, and Zn^{2+}. These ion exchanged zeolites are capable of producing fuels with a total sulfur concentration less than 1 ppmw. In particular, the Cu(I)-Y zeolite (vapor phase ion exchanged, VPIE) exhibits the highest sulfur selectivity and capacity.[1,15,17] Recently experiments in our laboratory showed that Pd-based sorbents have higher sulfur capacities than Cu(I)-Y.[22] In addition, our previous studies have shown that activated carbon used as a guard bed can improve the adsorptive performance of Cu(I)-Y adsorbent.[12,15]

Equilibrium isotherms and heats of adsorption are important parameters for the design of adsorption processes. The shape of an isotherm provides significant information on the adsorption process. It indicates the nature and strengths of sorbate-sorbent and sorbate-solvent interactions and also the degree of energetic heterogeneity of the solid surfaces, which will provide useful information for the design of selective adsorbents. In

our previous studies,[23-24] vapor phase adsorption isotherms were investigated to understand the interaction between benzene/thiophene and various kinds of sorbents, including Ag-Y, Cu-Y, Na-Y, H-USY, Na-ZSM-5, activated carbon, and modified activated alumina. Ng et al.[25-26] studied the adsorption of thiophenic compounds in normal alkane solvents on NaY zeolite using flow calorimetry and thermogravimetric analysis.

Although there are number of organic sulfur compounds present in the fuels, aromatics sulfur compounds such as thiophene (T), benzothiophene (BT), dibenzothiophene (DBT) and methyl substituted benzothiophenes are of primary concern. In this work, a systematic study of the adsorption isotherms and heats of "refractory" benzothiophene type sulfur compounds on Cu(I)-Y (VPIE) and $PdCl_2$/AC sorbents from the liquid phase has been carried out. N-octane was chosen as the solvent. Vapor-phase adsorption isotherms of pure-component n-octane and thiophene were also measured. A simple theory for the relationship between the heat of adsorption from vapor phase and that from liquid solution was proposed. A fair agreement between the theory and experiment obtained. The simple theory is useful for the design of adsorption of liquid solutions from pure compound vapor-phase data.

2. Experimental Method

2.1 Preparation of Sorbents

The starting adsorbent material used in this study were type-Y zeolites (NH_4-Y, Si/Al=2.43, in powder form, Strem Chemicals) and activated carbon (type PCB, Calgon Carbon Corporation). The activated carbon was first ground and sieved to 100-140 mesh particle sizes. H-Y zeolite was obtained by calcination of NH_4-Y in dry air at 450℃ at 1 ℃/min.

Cu(I)-Y: Cu(I)Y was prepared by vapor phase ion exchange of H-Y zeolite following procedures reported previously.[16,20] Layers of H-Y zeolite and CuCl (99.995+%, Sigma-Aldrich) were loaded into a reactor each separated by thin quartz wool walls. The reactor was heated in dry helium, from room temperature to 200 ℃ at 1 ℃/min and the temperature held at that point for 5 h. Afterward, the temperature was slowly increased to 675 ℃ and kept for another 10 h. The zeolite was then treated in oxygen at 200 ℃ for 4 h before cooling down to room temperature to a stable Cu^{2+} state.

$PdCl_2$/AC: The activated carbon was impregnated with $PdCl_2$ (99.9+%, Sigma-Aldrich). A known amount of $PdCl_2$ (1.7g) was magnetically stirred in 1M HCl aqueous solution of 15 cm^3 under dry helium surroundings at room temperature, and then 4 g activated carbon was added to the mixture. The carbon was impregnated with the solution for 24 h. The sample was then washed with deionized water until the pH of the water became ~ 5.0, and the sample was dried at 100 ℃ for 48 h. Before the adsorption experiment, the sorbent was activated *in situ* in a quartz adsorber under ultra-pure helium at 120 ℃ at 1℃/min and the temperature held at that point for 10 h.

2.2 Characterization of sorbents

The BET surface areas of the samples were measured by physical adsorption of N_2 at 77K using Micromeritics ASAP 2010. The elemental analysis of Cu(I)-Y and $PdCl_2$/AC were reported previously.[1,22] All thiophene, benzothiophene, 2-methyl benzothiophene dibenzothiophene and n-octane were purchased from Sigma-Aldrich and were used without further purification.

2.3 Adsorption procedure

Adsorption isotherms were measured by a batch method. Binary solutions containing n-octane and a sulfur compound of different concentrations (ranging from 1-200 ppmw-S) was used. The solution (3 cm^3) and the sorbent (30-50 mg), after *in situ* activation pretreatment, were mixed in a tubular vial (10cm^3 volume) equipped with a magnetic stirrer. The vial was then sealed and placed in a thermostatted bath with stirring for a desired equilibrium time at 20 ℃ and 50 ℃. In each case, a control vial with the same amount of solution but without any adsorbent was also placed in the same bath. The liquid phase was filtered with Whatman Grade 1 filter paper after equilibrium. The sorbate concentrations in the filtrate were determined by a gas chromatograph which is described below, and the amount of sulfur removed was calculated by comparing the sulfur content in the solution with that in the control vial.

Single component vapor-phase isotherms for n-octane and thiophene were measured at 90 ℃, 120 ℃ and 160 ℃ using standard gravimetric methods. A Shimadzu TGA-50 automatic recording microbalance was employed. Helium (pre-purified grade, Metro welding, 99.995%) was used as the carrier gas and was first passed through two consecutive gas-wash bottles (to ensure saturation), which contained octane (Aldrich, >99%) or thiophene (Aldrich, >99%). After the concentration had been diluted to the desired value by blending with additional helium, the mixture was directed into the microbalance.

Isosteric heats of adsorption (ΔH_{ad}) were calculated using the Clausius-Clapeyron equation from vapor-phase isotherms at different temperatures:

$$\Delta H_{ad} = -RT^2 \left(\frac{\partial \ln p}{\partial T} \right)_{q_s} \quad (1)$$

where q_s is the adsorbed amount (mmol-S/g-sorbent), p is the partial pressure of the sorbate, T is the adsorption temperature (K) and R is the gas constant. For liquid-solid adsorption the Clausius-Clapeyron equation should be:

$$\Delta h_{ad} = -RT^2 \left(\frac{\partial \ln C}{\partial T} \right)_{q_s} \quad (2)$$

where C is the equilibrium concentration of sulfur compound at temperature T.

2.4 Gas chromatograph analysis

All of the samples collected during the isotherms experiments were analyzed using a Shimadzu GC-17A v3 unit equipped with an EC-5 capillary column and a flame photometric detector. More details on the GC sulfur analysis could be found elsewhere.[13,16]

3. Results and Discussion

3.1 Sorbent preparation

The BET surface areas, pore volumes, and the median pore widths of the sorbent samples were measured by physical adsorption of N_2 at 77K using Micromeritics ASAP 2010. The results are shown in Table 1.

As mentioned, the sorbents were carefully activated *in situ*, to avoid any exposure to moisture. For the Cu(II)-Y, the activation was performed at 450℃ in helium to promote auto-reduction of Cu^{2+} species to Cu^{+}, which is needed for π-complexation. Auto-reduction of cupric ions to cuprous ions in zeolites has been reported by several groups.[27-29] Larsen et al. reported that about 40% of the cupric ions in Cu-ZSM-5 were reduced

under helium at 410℃.[30] Electron paramagnetic resonance studies by Takahashi et al. showed that 50% of Cu^{2+} in Cu(II)-Y zeolite was reduced under vacuum or helium at 450 ℃ after 1 h treatment.[23] GeDeon et al. found that treatment in helium under similar condition for 12 h yielded 75% auto-reduction.[31] In previous studies of our group, the reduction of Cu^{2+} to Cu^{+} was carried out in He at 450℃ for 18 h, which led to good results for fuel desulfurization.[17,19-20] It is clear that the treatment time plays a crucial role in full reduction to Cu(I). Figure 1 shows the equilibrium adsorption isotherms of thiophene on Cu(I)-Y samples subjected to different reduction times. It can be seen that adsorption capacity increased with the reduction time. The adsorption amount on the sample treated for 5 h was nearly half of that treated for 10 h, while little additional increase occurred beyond 10 h. Thus, the auto-reduction time of Cu(II)-Y to Cu(I)-Y was fixed at 10 h in this work.

3.2 Adsorption isotherms

The rates of adsorption from all binary solutions were fairly rapid, with that on $PdCl_2$/AC being slightly more rapid than Cu(I)-Y. In all cases, 2 h was adequate for reaching equilibrium.

The equilibrium isotherms for the adsorption of the four sulfur compounds from their binary solutions in *n*-octane on Cu(I)-Y zeolite and $PdCl_2$/AC are shown in Figures 2 and 3. The equilibrium data was fitted to the Langmuir-Freundlich single solute isotherm,[23] which has the form:

$$q_s = \frac{kQ_m C^{1/n}}{1 + kC^{1/n}} \qquad (3)$$

where Q_m is its maximum adsorption capacity, k is the Langmuir-type constant, and the exponent n indicates the heterogeneity of the site energies. The fitting range was from 0 to 200 ppmw-S per gram of sorbent. The fitted parameters for the Langmiur-Freundlich equation are given in Table 2.

The BET surface area of the $PdCl_2$/AC was 758 m^2/g. The content of the impregnated $PdCl_2$ was 19.7wt%. The molecular area for a monolayer of $PdCl_2$ could be estimated from its crystallographic data. Thus, at the maximum, only 18% of the surface of the $PdCl_2$ /AC was covered by $PdCl_2$, while the rest was activated carbon.

Adsorption of sulfur compounds from liquid 'fuels' on carbon has been studied previously.[1, 4, 32] Although various carbons could selectively adsorb thiophenic sulfur, the selectivity was not high enough because early breakthrough of small sulfur concentration occurred.[1] However, the sulfur capacities were high because of their large surface areas. Haji and Erkey reported data on adsorption of DBT/n-hexadecane on carbon aerogels,[4] and Zhou et al. reported data on adsorption of various sulfur compounds from a model diesel fuel.[32] The model diesel contained over 10 different compounds, and will not be compared here. Comparing the results in Figures 2 and 3 with that on aerogels, it is seen that the amounts adsorbed DBT were significantly higher on the π-complexatrion sorbents. More specifically, the amount of adsorbed DBT increased by 7-fold by impregnation of $PdCl_2$ on the carbon, due to π-complexation.

The unexpected result from Figures 2 and 3 was on the relative orders of the strengths of adsorption of different sulfur compounds on the two sorbents. Our molecular orbital calculations on the π-complexation bonds between these thiophenic compounds and these two sorbents (i.e., $PdCl_2$ and Cu-Y) were given in Ref. [22]. From these

calculations, it is known that the π-complexation bonds with Cu(I)-Y were stronger than that with $PdCl_2$, and that the relative order was: DBT > 2-MBT > BT > T.[22] Figure 2 shows that this order was indeed followed for $PdCl_2$/AC. However, for Cu(I)-Y, the order was BT > 2-MBT > DBT > T, as shown in Figure 3. The contrasting orders pointed to the fact that, beside the sorbate-sorbent bond energy, other factors such as sorbate (or solute)-solvent interaction and solvent-sorbent interaction are also important in adsorption from liquid solutions. This aspect was also pointed out earlier by Ng and coworkers in discussion of their calorimetric results on heats of adsorption from solutions.[25, 26] It should also be noted that the same order of adsorption strengths on $PdCl_2$/AC was also reported for activated carbon (without impregnation).[32] The contrasting orders will be explained by a simple theory below.

3.3 Heats of adsorption from binary liquid solutions

Figures 4, 5 and 6 show the equilibrium isotherms of thiophenic sulfur compounds on $PdCl_2$/AC at 20℃ and 50℃. Similar results are shown in Figures 7 and 8 for Cu(I)-Y. The data were fitted by the Langmuir-Freundlich equation, and the fitting parameters are included in Table 2. Heats of adsorption were calculated using the Clausius-Clapeyron equation (Eq. 2) from isotherms at two different temperatures, and are summarized in Table 4. Point B is the point at which the linear section of the isotherm commences, near the knee of the isotherm. It is often considered the point at which the first monolayer has been completed. The amount adsorbed at this point can be used to reflect the monolayer adsorption capacity of sorbent and to determine the sorbent surface area. The non-calorimetric determination of the adsorption enthalpy yields isosteric heats (Δh_{ad}) which are differential heats.

The heat of adsorption tends to decrease as the loading is increased in single component vapor phase adsorption.[23] The overall heat of adsorption of thiophene (vapor phase adsorption) on activated carbon ranged from 23.9 kcal/mol at 0.5 mmol-S/g sorbent loading to 8.0 kcal/mol at 3 mmol-S/g sorbent loading, the overall heat of adsorption of thiophene on Cu(I)-Y (liquid-phase ion exchange, LPIE) ranged from 22.4 kcal/mol at 0.5 mmol-S/g sorbent loading to 20.8 kcal/mol at 3 mmol-S/g sorbent loading. [23] Ng et al.[26] reported that the average heat of adsorption was 20.9 kJ/mol on NaY for thiophenic S compounds in hexadecane based on the liquid calorimetric studies. It should be noted that the heat measured from flow calorimetry is an integral heat. From Figures 9 and 10, it is interesting to note that all the isosteric heats of adsorption had the tendency to decease first and then increased as the loading was increased for both sorbents, with the only exception for 2-MBT and DBT on Cu(I)-Y, where the isosteric heat decreased with increased loading. This phenomenon is consistent with most other systems.[33-35]

For small uptakes, the isosteric heat of adsorption generally decreased rather strongly with the amount adsorbed, indicating strong site heterogeneity, particularly for Cu-Y in which the faujasite framework contained cation sites of different energies. At intermediate uptakes, the isotherms became almost horizontal and thereafter ($-\Delta h_{ad}$) might actually increase, an effect ascribed to by sorbate-sorbate interactions as the intracrystalline fluids became denser.

The integral heat of adsorption, $\Delta\tilde{h}$, is related to the differential heat of adsorption (Δh_{ad}) for liquid-phase adsorption (or $\Delta\tilde{H}$ related to differential heat of adsorption ΔH_{ad} for vapor-phase adsorption) by the relation:

$$\Delta\tilde{h} = \frac{1}{q_s}\int_0^{q_s} \Delta h_{ad}\, dq_s \qquad (4)$$

where q_s is the adsorbed amount, same as in Equation (2). The integral heats of adsorption as a function of amount adsorbed for the thiophenic sulfur compounds on the two sorbents calculated using Equation (4) are also shown in Figures 9 and 10 for comparison. It can be seen that the integral heats for all thiophenic sulfur compounds remained nearly constant. This coincided with the results on sorbents such as ion-exchanged zeolites and activated carbon which also had heterogeneous sites.[34-35] The calculated results of the heats of adsorption are listed in Table 4. These results indicated that the adsorption strengths decreased in the order of: benzothiophene (BT) > 2-methyl benzothiophene (2-MBT) > dibenzothiophene (DBT) > thiophene (T) for Cu(I)-Y, while followed the order of: dibenzothiophene (DBT) > 2-methyl benzothiophene (2-MBT) > benzothiophene (BT) > thiophene (T) on $PdCl_2$/AC.

3.4 Heats of adsorption from vapor phase

In order to understand the roles played by the solvent-sorbent interaction and sorbate-solvent interaction in the adsorption from binary liquid solutions, pure-component isotherms for thiophene and *n*-octane were measured at different temperatures using a standard gravimetric method. The results are shown in Figures 11 and 12. Only thiophene was used because the other sulfur compounds are solid at room temperature and the measurements of adsorption from vapor phase for such low volatile compounds are extremely difficult. By comparing Figure 11 with Figure 12, it is seen that $PdCl_2$/AC has a higher adsorption capacity than Cu(I)-Y zeolite for the n-octane, which was due to the larger BET surface area of $PdCl_2$/AC (Table 1) for the purely physical adsorption for the n-octane molecule. However, for adsorption of thiophene, Cu(I)-Y zeolite showed a

significantly higher adsorption capacity than $PdCl_2$/AC, which indicated the adsorption of thiophene mainly via π-complexation.[21] Figures 13 and 14 show the heats of adsorption for n-octane and thiophene on these two sorbents, which are also included in Table 3. It is clear that the heats of adsorption of thiophene were much higher for Cu(I)Y than that on $PdCl_2$/AC, because of π-complexation. As mentioned, the surface of the $PdCl_2$/AC was mainly activated carbon with less than 20% being covered by $PdCl_2$. Thus, the heats were overall values for both carbon and $PdCl_2$. It is clear that ΔH_{ad} calculated with Eqn. (1) was sensitive to q_s, and the value of the integral heat $\Delta\tilde{H}$ was rather independent of q_s. There was also additional heat released with the increased loading due to increased sorbate-sorbate van der Waals interactions.

3.5 **Relationship between adsorption from vapor phase and from liquid solution**

Adsorption bond energies can now be calculated for both physical adsorption (by Monte Carlo simulation) and chemisorption (by *ab initio* molecular orbital theory), and these energies are approximately equal to the heats of adsorption.[36] The heat of adsorption provides the basic information for the adsorption process, which is also important in design for practical applications. For π-complexation systems involving the thiophenic compounds, in particular, the heats of adsorption are in general agreement with the adsorption bond energies that are calculated from molecular orbital theory. [6, 20, 22-24, 36] The heats of adsorption are almost always measured by pure-component adsorption from vapor phase. The heats of adsorption follow the order of: dibenzothiophene (DBT) > 2-methyl benzothiophene (2-MBT) > benzothiophene (BT) > thiophene (T). For adsorption from binary liquid solutions, this order was followed by $PdCl_2$/AC, but not followed by Cu(I)-Y.

In order to explain this contrasting behaviors for the adsorption from solution by these two sorbents, a basic understanding of the relationship between pure-component adsorption from vapor phase and adsorption from liquid solution is needed. To our knowledge, such relationship has not been discussed in the published literature.

Pure-component vapor phase adsorption can be predicted once the sorbate-sorbent interaction potentials are known. Adsorption from the binary liquid solution is much more complex than that from the gas phase.[25, 26, 36] Adsorption of a solute (i.e., sorbate) from a binary solution depends on sorbate-sorbent, sorbate-solvent, sorbate-sorbate and solvent-solvent interactions, and these interactions are reflected by the overall heat of adsorption. When a solid is immersed in a dilute solution, neglecting the heat of dilution, the heat of immersion (i.e., molar immersion heat, h_i) is related to the integral heat of adsorption from the vapor ($\Delta\tilde{H}$) by: [38]

$$h_i = -\Delta\tilde{H} + \Delta H_L \qquad (5)$$

where ΔH_L is the heat of liquefaction.

For adsorption from a liquid solution, the overall heat of adsorption includes:

1. the exothermic wetting/adsorption of solvent;
2. the endothermic or exothermic energy for dissociating the solute (or sorbate) molecule from the solvent; and
3. the energy for displacement of the adsorbed solvent molecules by the solute molecules.

In these steps, (1) is represented by the heat of immersion, and (2) is the inverse of the heat of dissolution. In Ng's calorimetric measurements, the sorbent was first wetted

by pure solvent before the solution was introduced.[25,26] So the heats of adsorption that were measured reflected step (3).

Based on the analysis above and Eq. 5, the relationship between pure-component vapor-phase heat of adsorption ($\Delta\tilde{H}$) and the heat of adsorption from liquid solution ($\Delta\tilde{h}$) can be expressed as:

$$\Delta\tilde{h} = \Delta\tilde{H} - h_i - \beta H_s \qquad (6)$$

where

$\Delta\tilde{h}$: integral heat of adsorption of solute from liquid solution

$\Delta\tilde{H}$: integral heat of adsorption for pure-component vapor-phase adsorption

h_i: heat of immersion of solid

H_s: energy for dissociating solute molecule from solution

β: fractional constant, accounting for remaining interactions between the adsorbed molecule with solvent.

For dilute solutions, as in our case, the immersion heat comes mainly from the solvent octane. Thus, h_i can be calculated using Equation (5) based on the integral heat of vapor phase adsorption of octane. The heat of liquefaction (ΔH_L) of n-octane is 38.54 kJ/mol. [39] The last term in Equation (6) is the difference in energies between the solute molecule (while in solution) and the molecule that is adsorbed. Since after adsorption, the adsorbed molecule remains in contact with some solvent molecules, the correction factor β is needed, which should be less than 1.

Before adsorption, all sulfur molecules are dissolved in the solvent, n-octane. Dissolution involves the following steps: (1) break up of solute-solute intermolecular bonds; (2) break up of solvent–solvent intermolecular bonds; (3) formation of a cavity in solvent phase large enough to accommodate the solute molecule; (4) vaporization of

solute into cavity of the solvent phase; and (5) formation of solute–solvent intermolecular bonds. Again, because of the low concentration of sulfur compounds in solution (< 200 ppmw-S), the sulfur molecule is in an environment of essentially pure n-octane molecules. Therefore, when a sulfur molecule is adsorbed onto the solid surface, it should first break the bonds with the surrounding solvent molecules, which is referred to as the cavity formation energy. This bond energy can be expressed by the familiar cohesive energy density (CED or c), which is the energy needed to remove a molecule from its nearest neighbors, and is defined by: [40]

$$CED = \frac{\Delta U_i}{V_i^l} \qquad (7)$$

where V_i^l is the liquid molar volume of pure liquid *i* at temperature T, and ΔU_i is equal to H_v - RT where H_v is the heat of vaporization, which is a measure of cohesive interactions in the liquid. The square root of the CED for liquid *i* is the Hildebrand solubility parameter for that liquid:

$$\delta = \sqrt{CED} \qquad (8)$$

Thus, ΔU_i can be calculated from the Hildebrand solubility parameter δ. However, the Hildebrand solubility parameter in regular solution theory reflects the overall energy for breaking the solvent-solvent interactions, being calculated from the vaporization enthalpy,[40] whereas for cavity formation only breaking a part of such interactions is required.

For binary mixtures of regular solutions, the cohesive energy density c_{12} reflects the intermolecular forces between molecules of components 1 and 2 , which may be related to c_{11} (the CED of pure component 1) and c_{22} (the CED of pure component 2) by [40]

$$c_{12} = (c_{11}c_{22})^{1/2}(1 - l_{12}) \tag{9}$$

where l_{12} is a binary parameter for nonpolar molecules, being either positive or negative, but is small compared with unity and is usually or the order of 10^{-2}.[40] It is essentially an empirical parameter and it depends on temperature.

Combining Eqs. (7), (8) and (9), the cohesive energy density c_{12} can be expressed by:

$$\begin{aligned} c_{12} &= \sqrt{c_{11}c_{22}}(1 - l_{12}) = \sqrt{\delta_1^2\delta_2^2}\,(1 - l_{12}) \\ &= \sqrt{\frac{\Delta U_1}{V_1^l}\frac{\Delta U_2}{V_2^l}}(1 - l_{12}) = \frac{\Delta U_{12}}{V_{12}^{\ l}}(1 - l_{12}) \end{aligned} \tag{10}$$

Here, $\Delta U_{12} = \sqrt{\Delta U_1 \Delta U_2}$, $V_{12}^{\ l} = \sqrt{V^l{}_1 V_2^{\ l}}$, $\delta_{12} = \sqrt{\delta_1\delta_2}$. The last term of Equation (6) which means the energy used to break up the interaction of solvent-solvent and solvent-sorbate can be expressed as:

$$\beta H_s = \beta\delta_{12}^2 V_{12}^l \tag{11}$$

where subscript 1 represents the solute (sulfur molecule), 2 represents the solvent n-octane and the fractional parameter β corrects for the partial dissociation of the solute molecule from the solvent upon adsorption.

The Hildebrand solubility parameter δ of thiophene can be calculated from its molar enthalpy of vaporization.[41] Whereas the δ of the other sulfur compounds in Eq. (10) and Eq. (11) can be estimated using Small's molar attraction constants combined with the thiophene molar attraction constant.[41] The results are given in Table 5.

Based on the above simple analysis, the relationship between the heats of adsorption from pure-component vapor phase adsorption and that for adsorption from binary liquid solutions were calculated using Eq. (6) and Eq. (11), and are summarized in Table 6.

Table 6 shows the prediction for heats of adsorption of pure-component sulfur compounds from vapor phase based on that from binary liquid solutions (in n-octane). From these results it is noted that when $\beta = 1$, meaning no correction for the cavity formation energy, the predictions by Equation (6) for thiophene adsorption on both Cu(I)-Y and $PdCl_2$/AC are quite reasonable. The average errors of the predicted heats of adsorption for thiophene from the vapor phase on these two sorbents are 6% and 3%, respectively. The predicted vapor-phase heats of adsorption calculated by Eq. (6) are greater than that from experiments, reflecting that the correction parameter β is needed. The predicted order of heats of adsorption for pure-component vapor-phase adsorption followed the order: T < BT < 2-MBT < DBT for both sorbents. The predicted order is in agreement with the adsorption bond energies calculated from *ab initio* molecular orbital theory as well as the order determined from experimental fixed-bed adsorption breakthrough order.[22] As discussed above, the selectivity of adsorption from liquid solutions followed the order of: T < BT < 2-MBT < DBT for $PdCl_2$/AC, and T < DBT < 2-MBT < BT for Cu(I)-Y zeolite. Most significantly, the simple theory can explain and provides insight for the fact that these two contrasting orders yielded the same (and correct) order for pure-component vapor-phase adsorption, or vice versa.

In Table 6, if we take β=0.75 for Cu(I)-Y and 0.8 for $PdCl_2$/AC, the predicted results of heats of adsorption for these sulfur compounds had less errors compared with the values calculated from molecular orbital theory, except for thiophene. This result indicates that when thiophenic sulfur compounds were adsorbed from the liquid solutions, breakage of only parts of the cavity formation interactions were required, and this energy was affected by different sorbents and different sulfur components.

4. Conclusion

Adsorption isotherms for thiophenic sulfur compounds in binary solutions in n-octane were measured for two different sorbents (Cu(I)-Y zeolite and $PdCl_2$/AC) where the sulfur compounds were preferentially adsorbed by π-complexation interactions. The adsorption-selectivity increased in the order of T(thiophene) < BT(benzothiophene) < 2-MBT(2-methyl benzothiophene) < DBT(dibenzothiophene) for $PdCl_2$/AC, and T < DBT < 2-MBT < BT for Cu(I)-Y zeolite. Analysis of the heats of adsorption (including differential and integral heats) were in agreement with these selectivity orders. Cu(I)-Y had higher adsorption capacities for these sulfur compounds than $PdCl_2$/AC except for DBT. Pure-component vapor-phase isotherms were also measured for n-octane and thiophene.

A simple theory was formulated for the relationship between the heats of adsorption from liquid solution and that from vapor phase. Using this theory, prediction were made for the vapor-phase adsorption of the sulfur compounds from the data on adsorption from liquid solutions. The results showed that the heat of adsorption for pure-component sulfur compounds on both sorbents were agreement with the adsorption bond energies obtained from *ab initio* molecular orbital theory, i.e., T < BT < 2-MBT < DBT. Most significantly, the simple theory can explain and provides insight for the fact that the two seemingly contrasting orders for selectivities for adsorption from liquid solutions on the two different sorbents yielded the same (and correct) order for pure-component vapor-phase adsorption.

References

(1) Hernández-Maldonado, A. J.; Yang, R. T. *Catal. Rev.- Sci. Eng.* **2004**, *46*, 111-150.

(2) Hernández-Maldonado, A. J.; Qi, G. S.; Yang, R.T. *Appl. Catal. B* **2005**, *61*, 212-218.

(3) Kemsley, J. *Chem. Eng. News* **2003**, *81*, 40.

(4) Haji, S.; Erkey, C. *Ind. Eng. Chem. Res.* **2003**, *42*, 6933-6937.

(5) McKinley, S. G.; Angelici, R. J. *Chem. Commun.* **2003**, 20,2620-2621.

(6) Yang, R. T.; Hernández-Maldonado, A. J.; Yang, F. H. *Science* **2003**, *301*, 79-81.

(7) Weitkamp, J.; Schwark M.; Ernst S. *J.Chem.Soc., Chem. Commun* **1991**, 16, 1133-1134.

(8) Salem, A.S.; Hamid H.S. *Chem.Eng.Technol.***1997**, 20, 342-347.

(9) Irvine, R.L. Process for Desulfurizing Gasoline and Hydrocarbon Feedstocks; *U.S.Patent* 5,730,860, 1998.

(10) King, D.L.; Faz.C.; Flynn T. *SAE Paper* 2000-01-0002, Society of Automotive Engineers; Detroit,MI, 2000.

(11) Kim, J. H.; Ma X. L.; Zhou A. N.; Song C. S. *Catal. Today* **2006**, 111. 74-83.

(12) Song, C.S. *Catal.Today* **2003**, 86, 211-263.

(13) Velu, S.; Ma, X.L.; and Song, C.S. *Ind. Eng. Chem. Res.* **2003**, 42, 5293-5304.

(14) Jeevanandam, P.; Klabunde, K. J.; Tetzler, S. H. *Microporous Mesoporous Materials* **2005**, 79, 101-110.

(15) Yang, R. T.; Yang, F. H.; Hernández-Maldonado, A. J., Takahashi, A. Selective Sorbents for Purification for Hydrocarbons, *U.S. Patent* No. 7,029,574. **2006**; *U.S. Patent* No. 7,053,256. **2006**; *U.S. Patent* 7,094,333, **2006**.

(16) Hernández-Maldonado, A. J.; Yang, R. T. *J. Am. Chem. Soc.* **2004**, *126*, 992-993.

(17) Hernández-Maldonado, A. J.; Yang, R. T. *AIChE J*. **2004**, *50*, 791-801.

(18) Hernández-Maldonado, A. J.; Yang, R. T. *Angew. Chem. Int. Edit.* **2004**, 43, 1004-1006.

(19) Hernández-Maldonado, A. J.; Stamatis, S. D.; Yang, R. T.; He, A. Z.; Cannella, W. *Ind. Eng. Chem. Res.* **2004**, *43*, 769-776.

(20) Hernández-Maldonado, A. J.; Yang, F. H.; Qi, G.; Yang, R. T. *Appl. Catal. B* **2005**, *56*. 111-126.

(21) Hernández-Maldonado, A. J.; Yang, R. T. *Ind. Eng. Chem. Res.* **2003**, *42*, 3103-3110.

(22) Wang, Y.; Yang, F. H.; Yang, R. T. *Ind. Eng. Chem. Res.* **2006**, 45, 7649-7655.

(23) Takahashi A.; Yang F. H.; Yang R.T. *Ind. Eng. Chem. Res.* **2002**, 41, 2487-2496.

(24) Yang, R.T.; Takahashi, A.; and Yang, F.H. *Ind. Eng. Chem. Res.* **2001**, 40, 6236-6239.

(25) Ng, F. T. T.; Rahman, A.; Ohasi, T.; Jiang, M. *Appl. Catal. B* **2005**, 56, 127-136.

(26) Jiang, M.; Ng, F.T.T.; Rahman, A.; Patel,V. *Thermochimica Acta* **2005**, 434, 27-36.

(27) Turnes Palomino, G.; Bordiga, S.; Zecchina, A.; Marra, G. L.; Lamberti, C. *J. Phys. Chem. B* **2000**, 104, 8641-8651.

(28) Chao, C.C.; Lunsford, J.H. *J.Chem.Physic* **1972** , 57, 2890-2898.

(29) Jacobs, P.A.; Wilde, W.D.; Schoonheydt, R.A.; Uytterhoeven, J.B. *J. Chem. Soc., Faraday Trans. 1:* **1976**, 72, 1221-1230.

(30) Larsen, S.C.; Aylor, A.; Bell, A.T.; Reimer, J.A. *J. Phys. Chem.***1994**, 98, 11533-11540.

(31) Ge'De'on, A.; Bonardet, J.L.; Lepetit, C.; Fraissard, J. *Solid State Nucl. Mag* **1995**, 5,201-204.

(32) Zhou, A. N.; Ma, X. L.; Song, C. S. *J. Phys. Chem. B* **2006**, *110*, 4699-4707.

(33) Barrer, R.M. *Zeolites and Clay Minerals as Sorbents and Molecular Sieves*; Academic press: London , 1978; p 164

(34) Anderson, P.J.; Pethica, B.A. *Trans.Faraday Soc*. **1956**, 52,1080-1087.

(35) Shen, D.M.; Engelhard, M.; Siperstein, F.; Myers, A.L.; Bulow, B. A. *Zeolites and mesoporous materials at the dawn of the 21st century : proceedings of the 13th International Zeolite Conference*, Montpellier, France, 8-13 July 2001 ; edited by Galarneau,Amsterdam , New York : Elsevier, c2001,106-110.

(36) Yang, R. T. *Adsorbents: Fundamentals and Applications*; Wiley: New York, 2003; p. 344.

(37) Ferreira, A. F. P.; Mittelmeijer-Hazeleger, M. C.; Bliek, A. *Microporous Mesoporous Materials* **2006**, 91, 47-52.

(38) Zettlemoyer, A.C.; Pendleton, P.; Micale, F.J. *Symposium on Adsorption from Solution*, edited by Ottewill, R.H.; Rochester, C.H.; Smith, A.L. Academic Press : London , New York , 1983; p 113.

(39) Weast, R.C.; Lide, D.R. *Handbook of Chemistry and Physics* ; CRC press: Bocn Raton , Florida , 1989-1990; p c-681.

(40) Reid, R.C.; Prausnitz, J.M.; Poling, B.E. *The Properties of Gases and Liquids;* Fourth Edition, McGraw-Hill Book Company : New York, 1987; p 284

(41) Small, P.A. *J. Appl. Chem* 1953, 3, 71-80.

Table 1: Surface areas and pore analyses of sorbents

sample	S_{BET} $m^2.g^{-1}$	V_{mic} $cm^3.g^{-1}$	V_{max} $cm^3.g^{-1}$	median pore width, nm
Cu(I)-Y	420	0.194	0.207	0.871
$PdCl_2$/AC	758	0.270	0.375	0.997

Table 2: Parameters for Langmuir-Frenudlich Equation for Adsorption of Sulfur from Binary Solution

	solution (in n-octane)	Temp ℃	Q_m mmol.g^{-1}	k	n
Cu(I)-Y	thiophene	20	3.112	0.0248	2.807
		50	0.277	0.0552	1.203
	benzothiophene	20	6.048	0.0537	3.338
		50	4.234	0.0606	4.474
	2-methylbenzothiophene	20	4.968	0.0791	6.195
		50	3.295	0.0837	4.627
	dibenzothiophene	20	4.359	0.0582	4.421
		50	1.342	0.0398	1.694
$PdCl_2$/AC	thiophene	20	0.0987	0.00510	0.978
		50	0.0819	0.00345	0.979
	benzothiophene	20	3.912	0.0151	2.617
		50	0.403	0.0501	1.494
	2-methylbenzothiophene	20	4.976	0.0071	1.851
		50	2.126	0.0278	2.987
	dibenzothiophene	20	7.578	0.0203	1.922
		50	1.649	0.0289	1.382

Table 3: Parameters for the Langmuir-Frenudlich Equation for Vapor Phase Adsortpion

	sorbate	Temp ℃	Q_m mmol.g^{-1}	k	n
Cu(I)-Y	thiophene	90	10.6	1.24	6.03
		120	6.39	2.50	4.71
	n-octane	120	1.22	361	1.13
		160	1.21	178	1.20
$PdCl_2$/AC	thiophene	90	10.7	2.33	2.61
		120	4.86	5.22	2.24
	n-octane	90	2.66	4.27	3.23
		120	2.70	3.20	3.33

Table 4: Isosteric Heat (at Point B) and Integral Heat of Adsorption (kJ/mol) for Adsorption from Binary Solution in n-Octane and from Vapor-Phase[a, b, c]

binary solution in n-octane	$PdCl_2$/AC				Cu(I)-Y			
	T	BT	2-MBT	DBT	T	BT	2-MBT	DBT
$q_{s,B}$ (mmol-S/g)	0.017	0.14	0.2	0.6	0.15	0.6	0.46	0.43
$-\Delta h_{ad,B}$ (kJ/mol)	15.94	28.34	27.19	35.46	39.74	52.78	44.29	41.02
$-\Delta \tilde{h}_B$ (kJ/mol)	15.44	30.69	31.64	40.05	40.72	49.66	50.66	50.71
$-\Delta \tilde{h}_{average}$ (kJ/mol)	15.76	30.21	30.07	47.05	42.58	50.34	48.02	47.88

vapor phase [d]	$PdCl_2$/AC		Cu(I)-Y	
	T	Octane	T	Octane
$q_{s,B}$ (mmol-S/g)	2.5	1.3	3.8	0.8
$-\Delta H_B$ (kJ/mol)	74.82	26.95	88.78	18.24
$-\Delta \tilde{H}_B$ (kJ/mol)	62.63	24.13	84.19	15.59
$-\Delta \tilde{H}_{average}$ (kJ/mol)	66.11	22.44	96.04	15.07

a: the solution of liquid adsorption is sulfur component in octane.

b: B means at point B, from the isotherm at 20℃ for liquid phase adsorption and 90 ℃ for vapor phase adsorption.

c: T = thiophene, BT = benzothiophene, 2-MBT = 2-methyl benzothiophene, DBT = dibenzothiophene.

d: vapor phase adsorption is for pure component adsorption.

Table 5: Hildebrand Solubility Parameters of Thiophene Sulfur Compounds

	thiophene[a]	benzothiophene[b]	2-methylbenzothiophene[b]	dibenzothiophene[b]
($cal^{1/2}.cm^{-3/2}$)	**10.1**	**12.5**	**12.4**	**12.3**

a. Calculated from heat of vaporization, from [39]

b. Calculated by $\delta = \frac{D\sum G}{M}$, where D (density) , M (molecular weight) and molar attraction constant G of phenylene and $-CH_3$, from [39]. G of thiophene was from calculated from a.

Table 6: Prediction for heat of adsorption from vapor phase based on that from binary liquid solution using Eq. (6)

	sorbate [a]	$-\Delta\tilde{H}$ (kJ/mol),vapor phase, experiment		$-\Delta\tilde{H}$ (kJ/mol)[b],vapor phase, calculated		$-\Delta\tilde{H}$ [c] (kJ/mol)	ΔE [d] (kJ/mol)
		Point B	Average	Point B	Average	Average	
Cu(I)-Y	T	84.19	96.04	100.02	102.4	76.85	89.45
	BT			127.33	128.53	96.39	95.72
	2-MBT			132.2	130.08	97.56	96.56
	DBT			139.83	137.52	103.14	98.65
$PdCl_2$/AC	T	62.63	66.11	66.2	68.21	54.56	77.75
	BT			99.82	101.03	80.82	79.84
	2-MBT			104.64	104.76	83.81	86.53
	DBT			120.63	129.32	103.45	95.30

a: T = thiophene, BT = benzothiophene, 2-MBT = 2-methyl benzothiophene, DBT = dibenzothiophene.

b: β in eq. (6) take as 1.0 , i.e., no correction for cavity formation energy.

c: β in eq. (6) take as 0.75 for Cu(I)-Y and 0.8 for $PdCl_2$/AC for correction for cavity formation energy.

d: adsorption bond energies come from (22)

Figure Captions

Figure 1. Adsorption isotherms of thiophene in *n*-octane on Cu(I)-Y (VPIE) auto-reduced for different lengths of time: ◆, 1.6 h ; ＊, 5 h ; □ , 10 h ; ▲, 18 h.

Figure 2. Adsorption isotherms of thiophenic sulfur compounds in *n*-octane on $PdCl_2$/AC at 20 ℃. × , T ; ▲ , BT; □, 2-MBT; ◆, DBT; dash lines are fitted with Langmuir-Freundlich model.

Figure 3. Adsorption isotherms of thiophenic sulfur compounds in *n*-octane on Cu(I)-Y at 20 ℃ . ○ , T ; ＊ , BT; △ , 2-MBT; ◆ , DBT ; solid lines are fitted with Langmuir-Freundlich model.

Figure 4. Adsorption isotherms of thiophene in *n*-octane on $PdCl_2$/AC at different temperatures. ■, 20 ℃; ×, 50 ℃; solid lines are fitted with Langmuir-Freundlich model.

Figure 5. Adsorption isotherms of benzothiophene (BT) and 2-methyl benzothiophene (2-MBT) in *n*-octane on $PdCl_2$/AC at different temperatures. +, BT 20 ℃; ＊ , BT 50 ℃; ■ , 2-MBT 20 ℃; ○ , 2-MBT 50 ℃ ; solid and dash lines are fitted with Langmuir-Freundlich model.

Figure 6. Adsorption isotherms of dibenzothiophene in octane on $PdCl_2$/AC at different temperatures. ■, 20 ℃; △, 50 ℃; solid lines are fitted with Langmuir-Freundlich model .

Figure 7. Adsorption isotherms of T and BT in *n*-octane on Cu(I)-Y at different temperatures. △ , T 20 ℃; ●, T 50 ℃; ×, BT 20 ℃; □, BT 50 ℃; solid and dash lines are fitted with Langmuir-Freundlich model.

Figure 8. Adsorption isotherms of 2-MBT and DBT in *n*-octane on Cu(I)-Y at different temperatures. ●, 2-MBT 20 ℃; ◇, 2-MBT 50 ℃; , ■, DBT 20 ℃; ×, DBT 50 ℃; solid and dash lines are fitted with Langmuir-Freundlich model .

Figure 9. Heats of adsorption of thiophenic sulfur compounds on $PdCl_2$/AC as a function of adsorbed amount. ■, differential heat of adsorption ; ○, integral heat of adsorption.

Figure 10. Heats of adsorption of thiophenic sulfur compounds on Cu(I)-Y as a function of adsorbed amount . ■, differential heat of adsorption ; □, integral heat of adsorption .

Figure 11. Adsorption isotherms of *n*-octane on $PdCl_2$/AC and Cu(I)-Y at different temperatures. ○, Cu(I)-Y 120 ℃; △, Cu(I)-Y 160 ℃; ■, $PdCl_2$/AC 90 ℃; ×, $PdCl_2$/AC 120 ℃; solid and dash lines are fitted with Langmuir-Freundlich model .

Figure 12. Adsorption isotherms of thiophene on $PdCl_2$/AC and Cu(I)-Y at different temperatures. ○, Cu(I)-Y 120 ℃; △, Cu(I)-Y 90 ℃; ■, $PdCl_2$/AC 90 ℃; ▲, $PdCl_2$/AC 120 ℃; solid and dash lines are fitted with Langmuir-Freundlich model

Figure 13. Heats of adsorption of *n*-octane on $PdCl_2$/AC and Cu(I)-Y from vapor phase adsorption as a function of adsorbed amount. ■, differential heat of adsorption ; ○, integral heat of adsorption .

Figure 14. Heats of adsorption of thiophene on $PdCl_2$/AC and Cu(I)-Y from vapor phase adsorption as a function of adsorbed amount . ■, differential heat of adsorption ; ○, integral heat of adsorption .

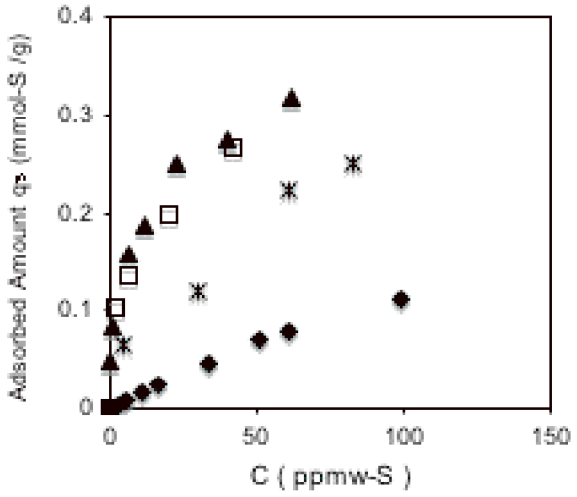

Figure 1. Adsorption isotherms of thiophene in *n*-octane on Cu(I)-Y (VPIE) auto-reduced for different lengths of time: ◆, 1.6 h ; ∗ , 5 h ; □ , 10 h ; ▲, 18 h.

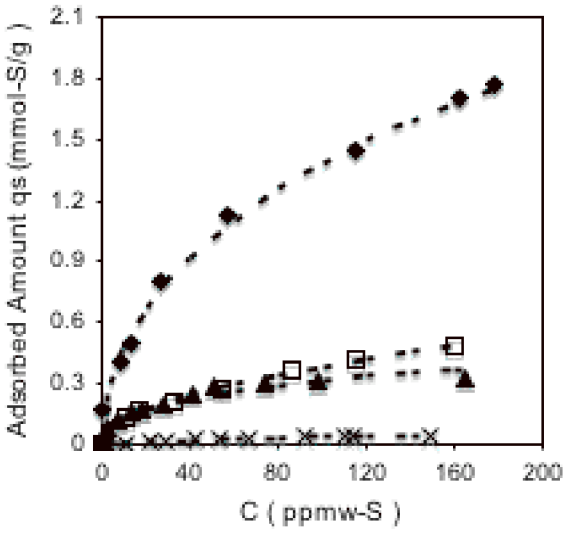

Figure 2. Adsorption isotherms of thiophenic sulfur compounds in *n*-octane on $PdCl_2$/AC at 20 ℃. × , T ; ▲ , BT; □, 2-MBT; ◆, DBT; dash lines are fitted with Langmuir-Freundlich model.

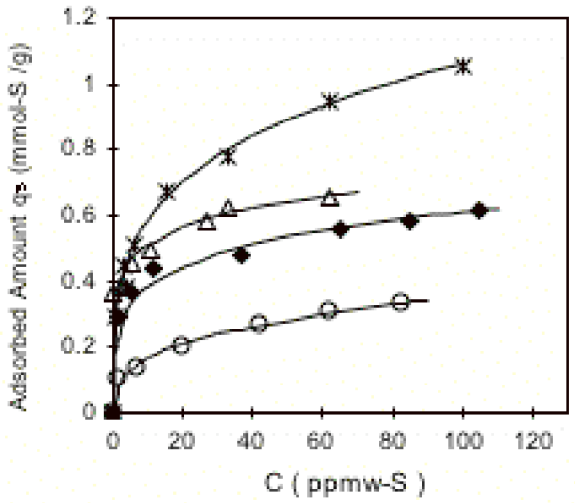

Figure 3. Adsorption isotherms of thiophenic sulfur compounds in *n*-octane on Cu(I)-Y at 20 ℃ . ○ , T ; ＊ , BT; △ , 2-MBT; ◆ , DBT ; solid lines are fitted with Langmuir-Freundlich model.

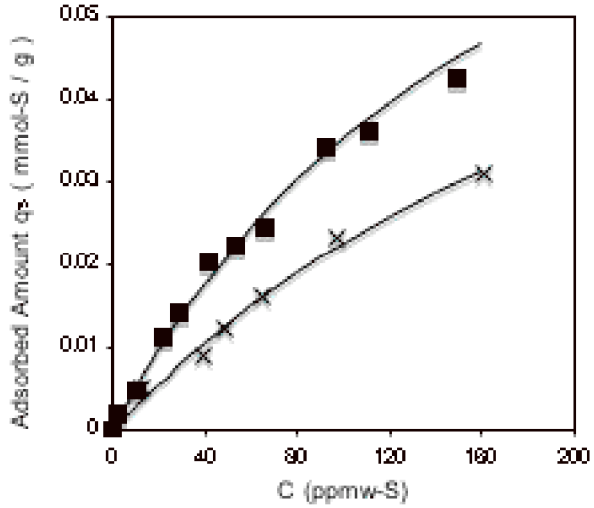

Figure 4. Adsorption isotherms of thiophene in *n*-octane on $PdCl_2$/AC at different temperatures. ■, 20 ℃; ×, 50 ℃; solid lines are fitted with Langmuir-Freundlich model.

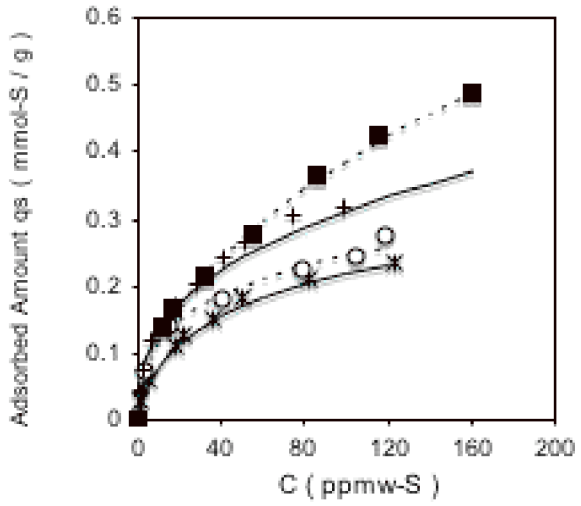

Figure 5. Adsorption isotherms of benzothiophene (BT) and 2-methyl benzothiophene (2-MBT) in *n*-octane on $PdCl_2$/AC at different temperatures. +, BT 20 ℃; ＊, BT 50 ℃; ■, 2-MBT 20 ℃; ○, 2-MBT 50 ℃; solid and dash lines are fitted with Langmuir-Freundlich model.

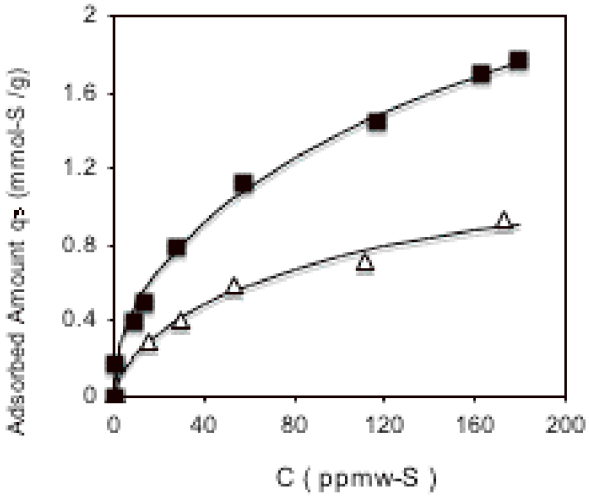

Figure 6. Adsorption isotherms of dibenzothiophene in octane on $PdCl_2$/AC at different temperatures. ■, 20 ℃; △, 50 ℃; solid lines are fitted with Langmuir-Freundlich model .

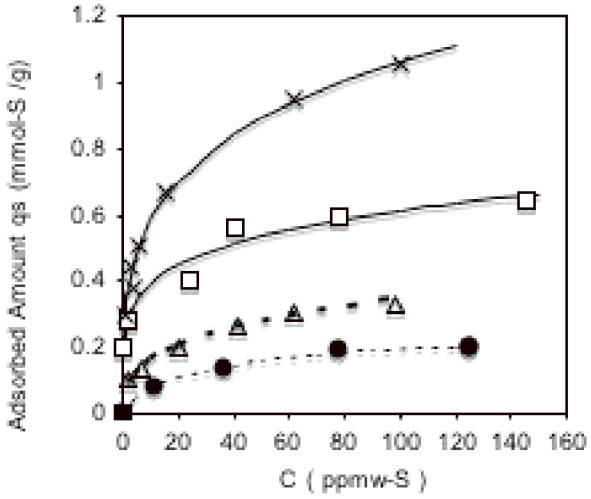

Figure 7. Adsorption isotherms of T and BT in *n*-octane on Cu(I)-Y at different temperatures. △ , T 20 ℃; ●, T 50 ℃; × , BT 20 ℃; □, BT 50 ℃; solid and dash lines are fitted with Langmuir-Freundlich model.

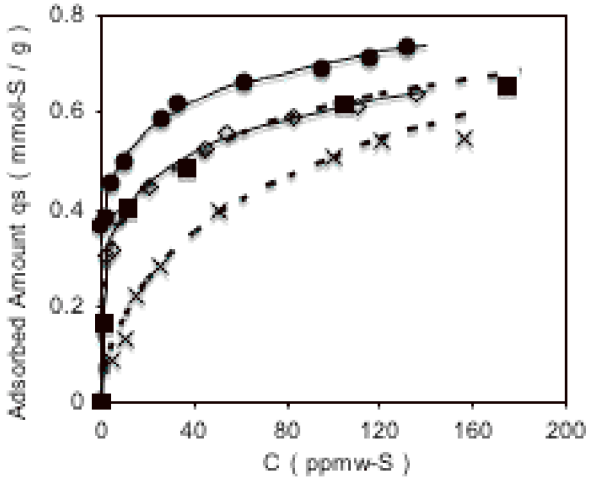

Figure 8. Adsorption isotherms of 2-MBT and DBT in *n*-octane on Cu(I)-Y at different temperatures. ●, 2-MBT 20 ℃; ◇, 2-MBT 50 ℃; , ■, DBT 20 ℃; ×, DBT 50 ℃; solid and dash lines are fitted with Langmuir-Freundlich model .

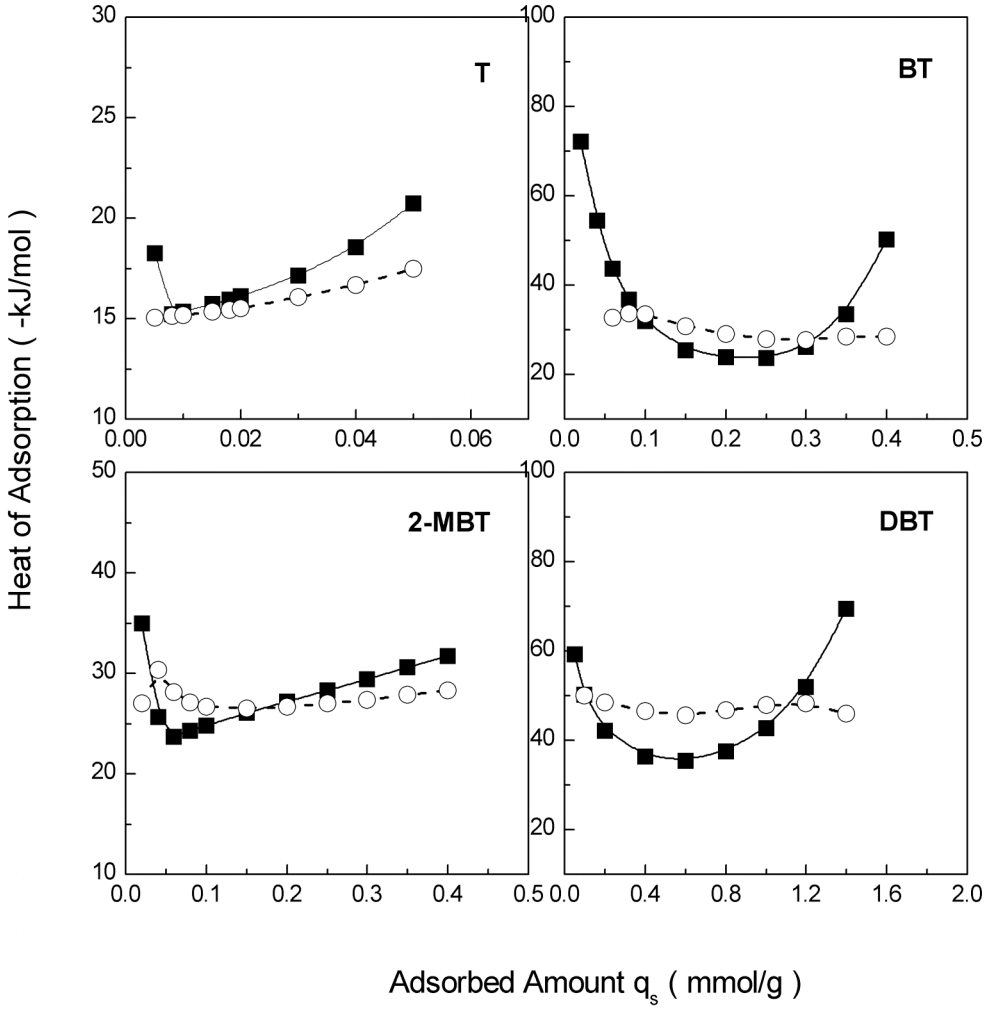

Figure 9. Heats of adsorption of thiophenic sulfur compounds on $PdCl_2$/AC as a function of adsorbed amount. ■, differential heat of adsorption ; ○, integral heat of adsorption.

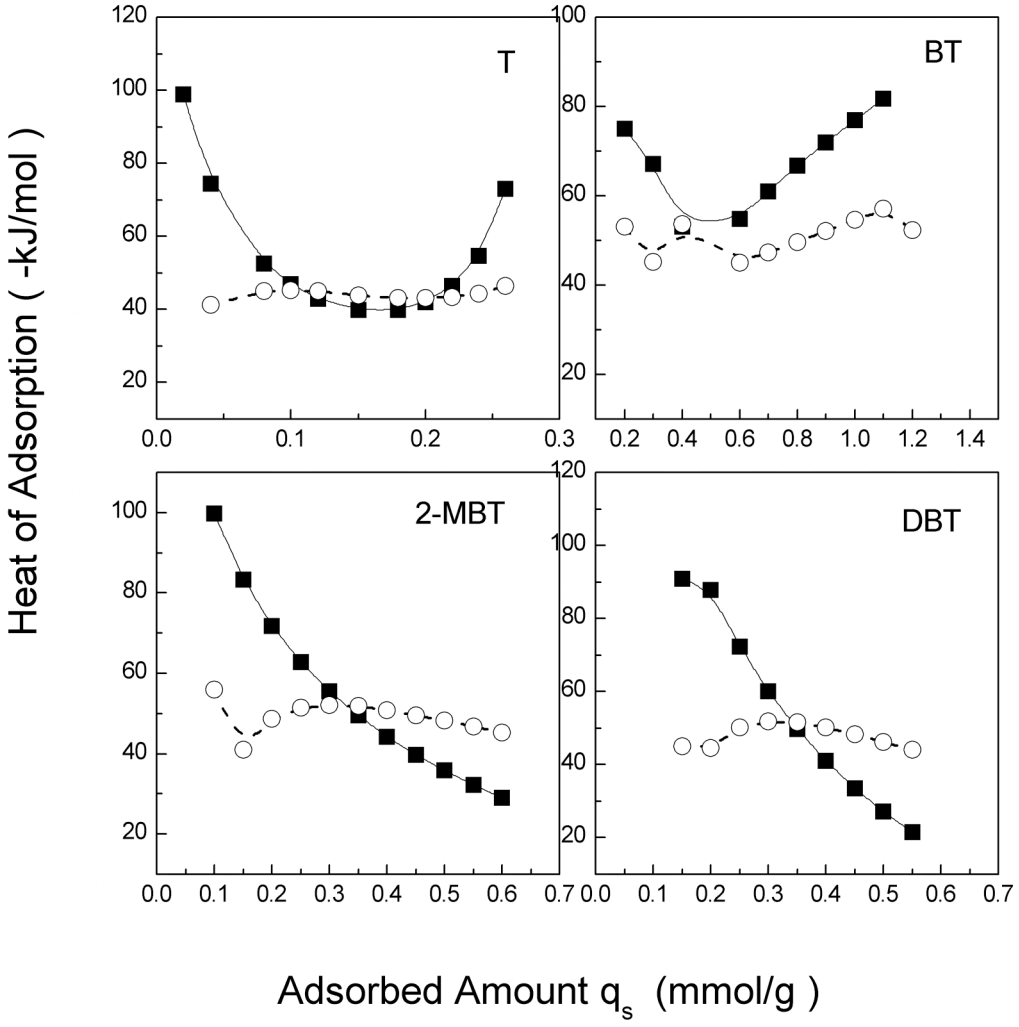

Figure 10. Heats of adsorption of thiophenic sulfur compounds on Cu(I)-Y as a function of adsorbed amount . ■, differential heat of adsorption ; □, integral heat of adsorption .

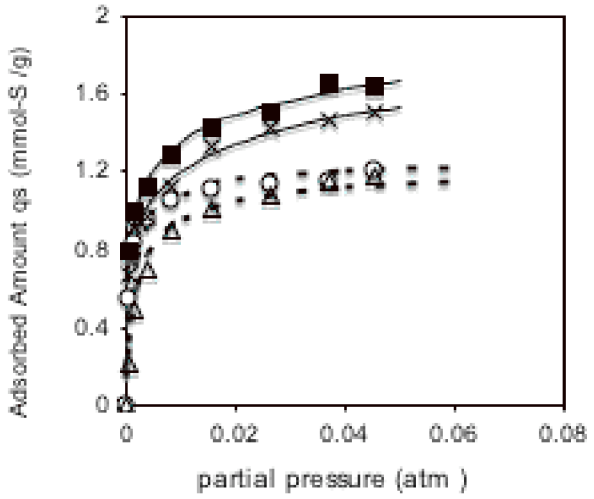

Figure 11. Adsorption isotherms of *n*-octane on $PdCl_2$/AC and Cu(I)-Y at different temperatures. ○, Cu(I)-Y 120 ℃; △, Cu(I)-Y 160 ℃; ■, $PdCl_2$/AC 90 ℃; ×, $PdCl_2$/AC 120 ℃; solid and dash lines are fitted with Langmuir-Freundlich model .

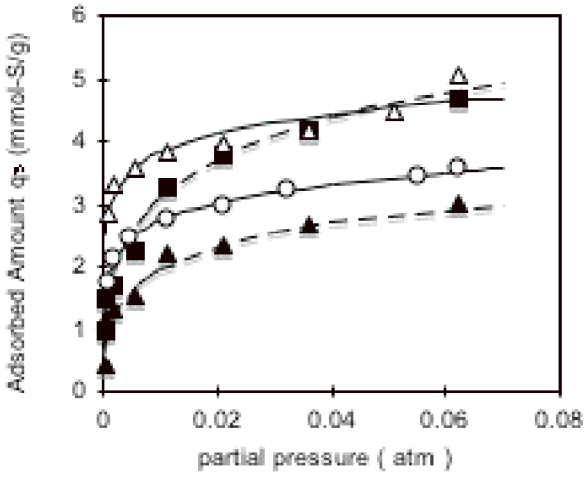

Figure 12. Adsorption isotherms of thiophene on $PdCl_2$/AC and Cu(I)-Y at different temperatures. ○, Cu(I)-Y 120 ℃; △, Cu(I)-Y 90 ℃; ■, $PdCl_2$/AC 90 ℃; ▲, $PdCl_2$/AC 120 ℃; solid and dash lines are fitted with Langmuir-Freundlich model

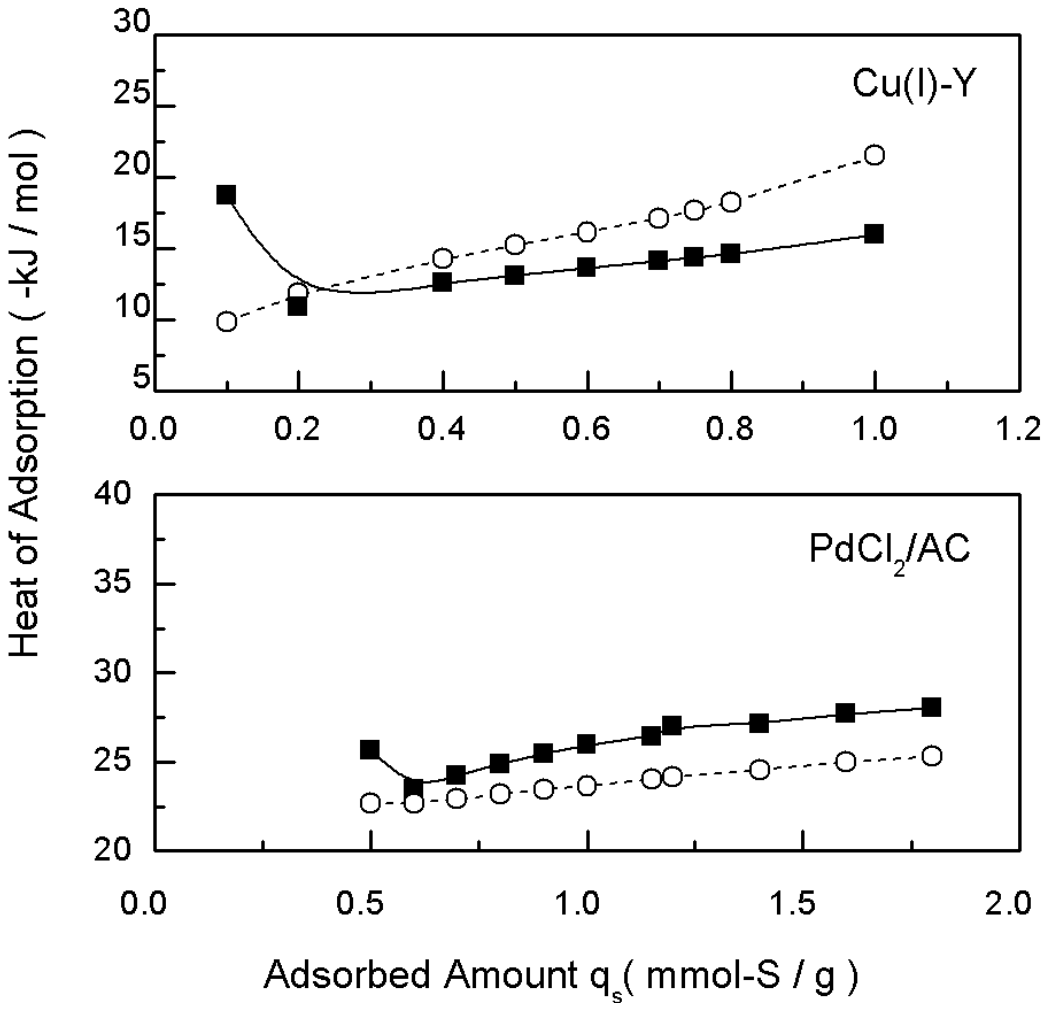

Figure 13. Heats of adsorption of *n*-octane on $PdCl_2$/AC and Cu(I)-Y from vapor phase adsorption as a function of adsorbed amount. ■, differential heat of adsorption ; ○, integral heat of adsorption .

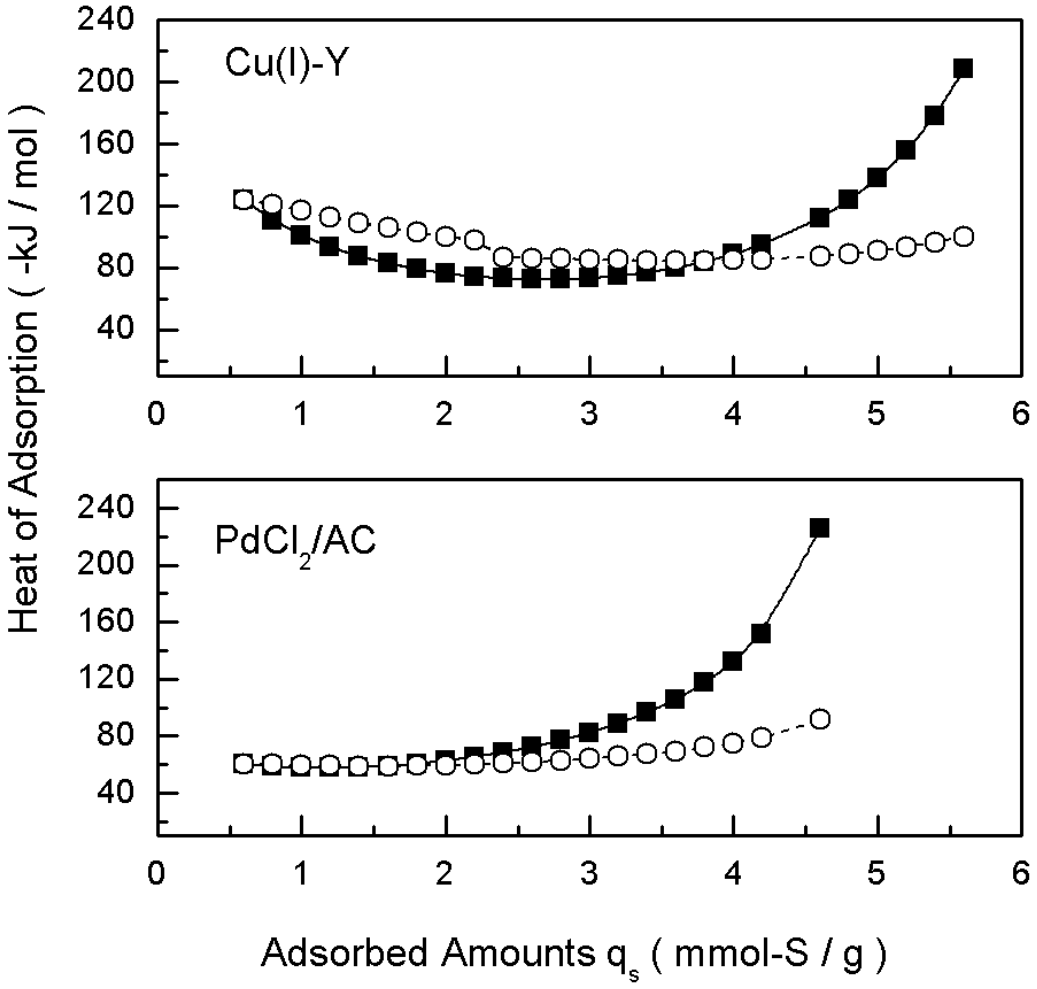

Figure 14. Heats of adsorption of thiophene on $PdCl_2$/AC and Cu(I)-Y from vapor phase adsorption as a function of adsorbed amount . ■, differential heat of adsorption ; ○, integral heat of adsorption .